LA-UR- 08-8098

Approved for public release; distribution is unlimited.

Title:	Stochastic pump effect and geometric phases in dissipative and stochastic systems
Author(s):	Nikolai Sinitsyn, 210821, CCS-3
Intended for:	J. Physics. A Math Theory Journal

Los Alamos
NATIONAL LABORATORY
EST. 1943

Form 836 (7/06)

REVIEW ARTICLE

Stochastic pump effect and geometric phases in dissipative and stochastic systems

N.A. Sinitsyn

Center for Nonlinear Studies and Computer, Computational and Statistical Sciences Division, Los Alamos National Laboratory, Los Alamos, NM 87545 USA

PACS numbers: 03.65.Vf

PACS numbers: 05.10.Gg

PACS numbers: 05.40.Ca

Abstract. The success of Berry phases in quantum mechanics stimulated the study of similar phenomena in many other branches of physics, including the theory of living cell locomotion and motion of patterns and topological defects in nonlinear media. Geometric phases recently were employed for systems operating in a strongly stochastic environment, such as molecular motors. We discuss geometric effects in purely classical dissipative and stochastic systems, including the latest progress in the theory of the stochastic pump effect, and its applications.

Contents

1. Introduction

The discovery of the Berry phase [1] revolutionized the way of thinking about many quantum mechanical phenomena. To recall it, imagine a quantum system with a Hamiltonian $\hat{H}(\mathbf{k})$, where $\mathbf{k}$ represents a set of externally controlled parameters. A quantum system is described by a complex valued wave function Ψ. However, the physical state of a system determines its wave function only up to an overall phase, because the gauge transformation

$$\Psi \to e^{i\phi}\Psi \tag{1}$$

defines the same physical state. Now assume that initially the wave function is one of the nondegenerate eigenstates of the Hamiltonian $\hat{H}$, and externally controlled parameters slowly change with time around a closed contour in the parameter space, so that at the end of the evolution they return to the inital values, as in Fig. 1. The adiabatic theorem of quantum mechanics guarantees that in the adiabatic limit the wave function will remain an instantaneous eigenstate of the Hamiltonian, and after completing the cycle, the physical state of the system should coincide with the initial one.

This theorem, does not mean that the phase of the wave function returns to the initial value. Careful examination shows that the phase picked up after a cyclic evolution can be written as a sum of two components

$$\phi = \phi_{\text{dyn}} + \phi_{\text{B}}, \tag{2}$$

where the dynamic phase $\phi_{\text{dyn}} = -\int_0^T E(t)dt$ appears even when parameters are fixed, while the other contribution (the Berry phase) has no stationary counterpart and is purely geometrical, in a sense that it depends only on the choice of the Hamiltonian and the path in the parameter space, but it does not depend explicitly on time of the evolution T and on the rate of "motion" along the contour, as long as the adiabatic approximation is considered. Given the dependence of the eigenstate $|u\rangle$ of the Hamiltonian on $\mathbf{k}$ in some gauge, the Berry phase reads

$$\phi_{\text{B}} = \oint_{\mathbf{c}} \mathbf{A}\cdot\mathbf{k}, \quad \mathbf{A} = \langle u|i\partial_{\mathbf{k}}u\rangle, \tag{3}$$

where $\mathbf{c}$ is the contour in the controlled parameter space, and $\mathbf{A}$ is called the Berry connection (see David J. Griffiths [2] for a pedagogical derivation). The cyclic

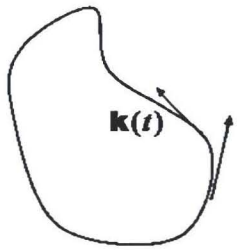

Figure 1. A closed contour in a controlled parameter space.

Berry phase is gauge invariant, and leads to measurable consequences, confirmed experimentally.

Berry's discovery had a rich prehistory. A number of effects in quantum mechanics had been related to the unusual phase evolution of the wave function even before

the Berry's contribution, as it is discussed in [3]. Even more historical examples can be found, for example, in the first efforts to create a semiclassical theory of the anomalous Hall effect [4, 5]. However, it was the Berry's work that unified all these known geometric effects under a universal theoretical framework, which was proved very successful for uncovering new effects and provided the theoretical groundwork for the entire brunches of physics such as the theories of the extraordinary Hall effects [6, 7, 8], the quantum theory of polarization [9], the topological quantum computation [10], and others.

The Berry phase is an example of the anholonomy effect encountered in the theory of differential equations. Anholonomy can be non-rigorously defined as not returning of vectors to the initial values after a parallel transport along a closed contour.

Are there effects in classical statistical physics, mathematically similar to Berry phases? Classical stochastic systems have a principal difference from quantum ones, which prevents direct analogies. While the state of a quantum system defines the wave function only up to an overall phase, a classical ergodic stochastic system can be described by a probability vector, without allowing any additional freedom in its definition. For example, consider a Markovian evolution, i.e a stochastic dynamics when the future evolution of the system is independent of the prehistory that brought a system into a given state. The evolution of the probability vector satisfies equations, reminiscent the quantum mechanical evolution. Fig. 2 shows the simplest such example. Lets compare a 2-state stochastic system and its quantum 2-state counterpart. In both cases the evolution is described by linear differential equations with 2×2 evolution matrices. In the quantum mechanical case, amplitudes u_1 and u_2 of two states evolve according to the Schrödinger equation

$$i\frac{d}{dt}\begin{pmatrix} u_1 \\ u_2 \end{pmatrix} = \begin{pmatrix} \epsilon_1(t) & \Delta(t) \\ \Delta^*(t) & \epsilon_2(t) \end{pmatrix}\begin{pmatrix} u_1 \\ u_2 \end{pmatrix}, \tag{4}$$

while the stochastic 2-state Markov chain evolution for probabilities p_1 and p_2 of the first and the second states reads

$$\frac{d}{dt}\begin{pmatrix} p_1 \\ p_2 \end{pmatrix} = \begin{pmatrix} -k_1(t) & k_2(t) \\ k_1(t) & -k_2(t) \end{pmatrix}\begin{pmatrix} p_1 \\ p_2 \end{pmatrix}. \tag{5}$$

In spite of the similarity of Eqs. (4) and (5), it is well known that a quantum mechanical cyclically driven 2-state system features the possibility of the geometric Berry phase but it is not true for its stochastic counterpart. At given values of parameters an ergodic Markov chain has a unique steady state. For slow evolution of parameters, the probability vector will simply follow the path of instantaneous steady state values, returning to the initial vector after parameters complete a full cycle.

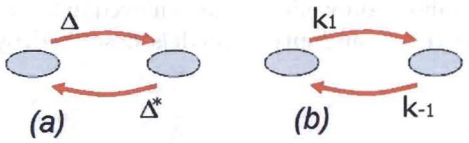

Figure 2. Two state (a) quantum and (b) stochastic systems.

This example shows that in some sense the Markovian evolution does not lead to adiabatic geometric phases. However, this conclusion is restricted only to the evolution of the state probability vector. There are other characteristics describing stochastic

processes. For example, one can consider stochastic transitions among 3 states in Fig. 3 and ask what is the probability that the system makes exactly n full cycles in a clockwise direction by the given time t. In the following sections we will derive the evolution equations for such and similar quantities and show that geometric phases do play an important role in their evolution.

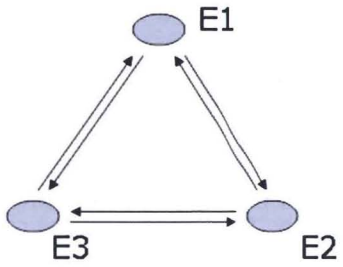

Figure 3. A 3-state Markov chain. This model can be considered as a "minimal" model to describe the stochastic behavior of a molecular motor in Fig. 12.

Anholonomies also play a central role in classical thermodynamics. Statistical properties of a system in the thermodynamic equilibrium can be specified by a set of parameters, such as the volume, the pressure and the temperature. Slow cyclic changes of these parameters merely produce cyclic changes of the equilibrium properties, so, as in the example of a 2-state Markov chain, a driven system returns to the initial state in a statistical sense by the end of a cycle. However, if one looks at the same process from a more general point of view, namely including effects of this process not only on the given system, but also on systems in contact with it, a cyclic adiabatic driving of parameters usually does not lead to the same finite state in the full phase space. Laws of thermodynamics predict that the system converts part of the absorbed energy into production of the work. Moreover, for adiabatically slow evolution the work depends only on the choice of the contour in the parameter space but does not depend on the rate of motion along this contour as long as the adiabatic approximation is valid, namely the work can be expressed as a contour integral over the path in the space of controlled parameters. For example, for a gas in a reservoir with variable volume V and temperature T, the work W produced per cycle is

$$W = \oint_{\mathbf{c}(T,V)} p(T,V) \cdot dV, \tag{6}$$

where $p(T,V)$ is the pressure.

A deep understanding of the anholonomy effects was achieved in the mathematical control theory [11]. Look e.g. at the input/output models described by differential equations

$$\dot{x}^i = f^i_j(\mathbf{x}) u_j(t), \tag{7}$$

where f_j are smooth functions of $\mathbf{x}$, and $u_j(t)$ represent controllable parameters. One can consider a simple cyclic evolution in the control parameter space by setting $u_1 = 1$, $u_i = 0$, for $i \neq 1$ during an infinitesimal time interval t. After this, one sets $u_2 = 1$, $u_i = 0$, for $i \neq 2$ during the following time interval $(t, 2t)$, then take $u_1 = -1$, $u_i = 0$, for $i \neq 1$ for $(2t, 3t)$, and finish with $u_2 = -1$, $u_i = 0$, for $i \neq 2$.

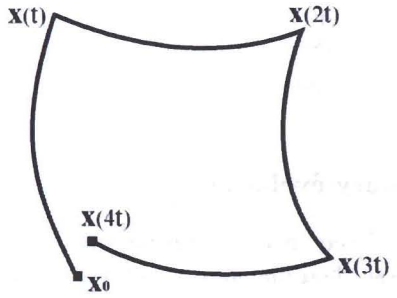

Figure 4. Trajectory of $\mathbf{x}$ in response to a periodic infinitesimal path in the space of controlled parameters $\{u_i\}$.

An easy perturbative calculation shows that after one such an infinitesimal cycle in the parameter space, the vector $\mathbf{x}$ does not generally return to the initial state but rather acquires an additional correction, namely

$$\mathbf{x}(4t) = \mathbf{x}_0 + \frac{t^2}{2}[f_2, f_1](\mathbf{x}_0) + \mathrm{O}(t^3), \tag{8}$$

where $[f_2, f_1]^i = (f_2^j \partial f_1^i/\partial x^j) - (f_1^j \partial f_2^i/\partial x^j)$ is called the Lie brackets of the vector fields f_1 and f_2. An important property of the Lie bracket operation is that its result cannot generally be expressed as a sum of the vectors inside the brackets. The study of such phenomena resulted in formulation of Frobenius and Chow theorems, playing a very important role in the theory of controllability [12].

The history of anholonomy effects in mathematics and statistical physics is very rich, with a number of important steps, which can be uncovered even before the 20th century. We will not provide an extensive discussion of many important contributions, as it would lead us way beyond the limits of our review. Instead, we will concentrate on applications of geometric phases to stochastic and dissipative processes, which attracted attention relatively recently, and were motivated partly by the success of the Berry phase in quantum mechanics. We attempted to make the review accessible to an audience not familiar with the mathematical theory of fiber bundles. This review is also not about a large body of work related to decoherence effects on quantum mechanical Berry phases or geometric phases in non-dissipative but chaotic systems [13]. We refer to books [14, 15] for a complementary introduction.

The structure of this review is as follows. Section II reviews extensions of the Berry phase idea to the non-unitary evolution. Section III describes geometric phases in dissipative systems with a continuous symmetry of steady state solutions, and their applications to the control over a pattern motion in a nonlinear media. Section IV briefly reviews the geometric theory of the living cell locomotion. In Section V we introduce the stochastic pump effect, and its relation to the geometric phases in the evolution of the moments generating functions (MGFs). In Section VI we show how such geometric phases can influence the kinetics of slow variables in a coarse-grained description. We show that they lead to effects similar to the Berry phase corrections in the quantum mechanical Born-Oppenheimer approximation. This section is technically more involved than others, however it can be safely omitted without complications for the rest of the review. In section VII we review the geomeric phases in the limit cycle evolution. Section VIII is about constraints that the detailed

balance conditions impose on geometric effects in systems driven close to or starting from the thermodynamic equilibrium. In Section IX we apply some of the discussed techniques to the theory of molecular motor operations, and we conclude in Section X.

2. Geometric phases in non-unitary evolution

Non-unitary evolution is often considered in quantum mechanical problems, where the coupling to the environment is described phenomenologically by introducing extra parameters in equations of motion for a density matrix or a wave function. In many physical problems one can encounter evolution equations, similar to quantum mechanical ones but with a non-Hermitian operator replacing the Hamiltonian. Examples can be found e.g. in electronic circuits [16], optics [17], acoustics [18]. Evolution of any dissipative system near a stable point or a limit cycle can be linearized, and thus acquire a form similar to the quantum mechanical Schrödinger equation for a state vector. Motivated by the success of the quantum mechanical Berry phase, many studies [19, 20, 21, 22] were devoted to the geometric phases in systems with non-Hermitian Hamiltonians. The models considered could generally be written in the form

$$\frac{d}{dt}|u\rangle = \hat{H}(\mathbf{k})|u\rangle, \tag{9}$$

where $\hat{H}$ is a $N \times N$ non-Hermitian matrix, and $|u\rangle$ is a N-vector.

Performing steps similar to the ones leading to the quantum mechanical Berry phase in the adiabatic limit, one can arrive to a similar result, namely, if the vector $|u\rangle$ at the initial moment of the evolution is one of the eigenstates of the matrix $\hat{H}(\mathbf{k})$, i.e.

$$\hat{H}|u(0)\rangle = \varepsilon|u(0)\rangle, \tag{10}$$

then after a slow cyclic evolution of parameters, the vector $|u\rangle$ generally returns to the initial one up to an overall prefactor, which can be split into a dynamic and geometric parts,

$$|u(T)\rangle = e^{-\oint_{\mathbf{c}} \mathbf{A}\cdot d\mathbf{k}} e^{\int_0^T dt\varepsilon(t)}|u(0)\rangle. \tag{11}$$

Berry [21] pointed that it is convenient to express the geometric phase by introducing also the left-eigenstates of the Hamiltonian $\mathbf{H}(\mathbf{k})$, such that

$$\langle u|\hat{H} = \langle u|\varepsilon. \tag{12}$$

The sets of eigenvalues for left and right eigenvectors coincide. For a non-Hermitian Hamiltonian, components of the left eigenvector are no longer complex conjugated components of the right eigenvector. In other respects there is a strong similarity with quantum mechanical Berry phases, e.g. the connection $\mathbf{A}$ can be written as

$$\mathbf{A} = \frac{\langle u|\partial_{\mathbf{k}} u\rangle}{\langle u|u\rangle}. \tag{13}$$

Non-Hermiticity of the Hamiltonian in (9) does not necessarily mean that $\hat{H}$ describes a dissipative evolution. The geometric phases with a non-Hermitian Hamiltonian that realizes transformations of the $SU(1,1)$ group (i.e. transformations that conserve $|z_1|^2 - |z_2^2|$ of a complex valued 2-vector (z_1, z_2)), have attracted considerable attention because of their applications to squeezed states [23, 24, 25, 26],

and a number of models in classical mechanics and optics [27, 28, 29]. The $SU(1,1)$ group is homomorphic to the 3-D Lorenz group. The corresponding geometric phase is responsible for a variety of relativistic effects, such as the Thomas precession [30, 31]. We refer the interested reader to the review [32]. More important for our subject is that the $SU(1,1)$ group is also isomorphic to the group $SL(2,R)$, of 2×2 matrices with real entries and the unit determinant. The $SL(2,R)$ evolution can describe a dissipative classical system, and corresponding geometric phases were studied both theoretically and experimentally in application to the light propagation through a set of polarizers [33, 34, 35]. Recently, the relation of this geometric phase to the stochastic pump effect was discussed in [36].

Similarly to the Berry phase, the geometric phase in Eq. (11) was generalized to the non-Abelian and non-adiabatic evolution [22, 37], and a number of applications were proposed, e.g. in optically active refracting media [21]. An intrinsic property of non-Hermitian Hamiltonians, not found in quantum mechanics, is the possibility of the so-called exceptional points in the spectrum. At such points not only eigenvalues but also eigenvectors of the Hamiltonian can merge. Encircling such points the eigenvectors acquire a geometric phase of a new type, studied theoretically in [38, 39, 40, 41], and observed in experiments [42, 43].

In spite of this progress, one can think that the geometric phase in dissipative evolution should be only a small effect on the background of the dynamic part in (11). The latter becomes either exponentially large or exponentially small with time. However, not all modes in dissipative evolution have to grow or decay exponentially. The situation changes when the matrix $\hat{H}$ has zero modes, i.e. one or several linearly independent states with a zero eigenvalue. If all other modes decay quickly, according to (11), the evolution of such a dissipative system in the adiabatic limit should be governed by the geometric phases. Another interesting possibility is when for fixed values of parameters, a system relaxes to a limit cycle. The corresponding eigenvalue has only nonzero imaginary part.

3. Control over pattern position and orientation

In early 90s, Landsberg [44, 45], and independently Ning and Haken [46, 47] suggested that geometric phases should generally appear in many classical systems, which can be described by a set of nonlinear differential equations with a one-parameter group of symmetry transformations. In such a system it is possible to reduce the evolution equations to the form, where one of the variables does not affect the evolution of the others, that is

$$\frac{d\mathbf{Y}}{dt} = \mathbf{F}(\mathbf{Y}, \lambda), \quad \frac{d\Theta}{dt} = H(\mathbf{Y}), \tag{14}$$

where Θ and the vector $\mathbf{Y}$ represent generalized coordinates of the system, $\mathbf{F}$ and H are nonlinear functions of the coordinate vector $\mathbf{Y}$, but not Θ. Assume that the system is initially at the steady state, and then the parameter vector λ becomes slowly changing with time. Landsberg considered the case when the evolution of the variable $\mathbf{Y}$ is dissipative so that at fixed parameters it always relaxes to a steady state value $\mathbf{Y}^*(\lambda)$, and thus for adiabatically slow evolution it simply follows the quasi-steady state trajectory up to a small non-adiabatic correction $\mathbf{Y}(t) \approx \mathbf{Y}^* + D\mathbf{F}^{-1}(\mathbf{Y}^*)\partial_t \mathbf{Y}^*$, where $D\mathbf{F}$ is the linearization of the vector function $\mathbf{F}$, and $D\mathbf{F}^{-1}$ is its inverse. This cannot be assumed about the variable Θ. Due to the symmetry $\Theta \to \Theta + \delta\theta$ of

Eq. (14), its steady state value is not specified. Hence Θ does not have to return to the initial value after parameters λ complete a full cycle. Landsberg showed in [45] that after a cyclic evolution, the variable Θ changes by an amount given by a trivial dynamic part $\Delta\Theta_{\rm dyn} = \int dt H(\mathbf{Y}^*(t))$ plus a geometric contribution

$$\Delta\Theta_{\rm geom} = \oint_{\mathbf{c}} \mathbf{A}\cdot d\lambda, \quad \mathbf{A} = DH(\mathbf{Y}^*)D\mathbf{F}^{-1}(\mathbf{Y}^*)\partial_\lambda \mathbf{Y}^*, \tag{15}$$

where $DH = \partial H/\partial \mathbf{Y}|_{\mathbf{Y}=\mathbf{Y}^*}$ is the linearization of the function H near the point $\mathbf{Y}^*$. To generalize (15) to continuous systems Landsberg considered the equations of the form

$$\frac{d\Psi(t,x)}{dt} = \hat{F}(x,\lambda)\Psi(t,x), \tag{16}$$

where $\hat{F}$ now is a nonlinear operator, which depends on time only through time-dependent control parameters λ, assuming invariance of the evolution equations (16) of some continuous symmetry transformation, for example the translation along the coordinate x.

Let $|\psi(x)\rangle$ be the stationary pattern profile, which is a time-independent solution of (16) for constant λ, and let $\langle v_0|$ be the zero mode of the conjugated to $D\hat{\mathbf{F}}$ operator $D\hat{\mathbf{F}}^+$, where $D\hat{\mathbf{F}}$ is the linearization of the operator $\hat{\mathbf{F}}$ near the solution $|\psi(x)\rangle$. Landsberg showed that after a cyclic evolution in the parameter space, the stationary pattern will change by a geometric shift $\Delta\Theta_{\rm geom}$ along the symmetry direction

$$\Delta\Theta_{\rm geom} = \oint_{\mathbf{c}} \mathbf{A}\cdot d\lambda, \quad \mathbf{A} = -\frac{\langle v_0|\partial_\lambda\psi\rangle}{\langle v_0|\hat{\chi}\psi\rangle}, \tag{17}$$

where $\hat{\chi}$ is the generator of the symmetry transformation.

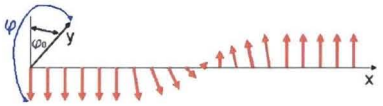

Figure 5. The wire with a hard anisotropy axis along it and a domain wall between two opposing magnetization directions. Easy axis anisotropy is perpendicular to the x-direction, and makes an angle ϕ_0 with a transverse y-axis.

Eq. (17) can be illustrated on a following simple example [48, 49]. Consider a 1D wire with a strong hard axis along it. This anisotropy favors the magnetization direction in the transverse plane, as shown in Fig. 5. We also assume the presence of a weak transverse anisotropy so that the magnetization energy is described by the energy functional

$$E \approx \int dx\{J(d\phi/dx)^2 + K\sin^2(\phi-\phi_0)\}, \tag{18}$$

where ϕ is the magnetization angle with a fixed transverse y-axis, and the parameter ϕ_0 is the angle that transverse anisotropy axis makes with y-axis (Fig. 5).

In the overdamped limit the evolution of the variable $\phi(x,t)$ reads

$$\alpha\partial_t\phi = -\frac{\delta E}{\delta\phi} = 2J\partial_x^2\phi - K\sin[2(\phi-\phi_0)], \tag{19}$$

where α is a damping constant. Note that Eq. (19) is invariant under the translation $x \to x - \delta x$, which justifies the applicability of the geometric theory of [44]. The generator of this symmetry is $\hat{\chi} = -\partial_x$.

At equilibrium, the ground state of (18) is doubly degenerate at $\phi = \phi_0$ and $\phi = \phi_0 + \pi$. Consider the domain wall solution connecting these two states

$$\phi^{\rm dw}(x;\phi_0,x_0) = \phi_0 + 2\tan^{-1} e^{(x-x_0)/\Delta}, \Delta = \sqrt{J/K_0}, \tag{20}$$

where x_0 and Δ can be called respectively the position and the size of the domain wall. Assume that the parameter ϕ_0 is slowly time-dependent, and changes through the values from 0 to 2π. i.e. the transverse anisotropy axis performs one rotation around the x-direction. One can realize this situation, for example, by physically rotating a wire. In our model ϕ_0 is the control parameter, and Eq. (17) gives

$$\delta x_0 = \oint \frac{\int_{-\infty}^{\infty} dx[v_0(x)\partial_{\phi_0}\phi^{\rm dw}(x)]}{\int_{-\infty}^{\infty} dx[v_0(x)\partial_x\phi^{\rm dw}(x)]} d\phi_0, \tag{21}$$

where $v_0(x)$ is the zero mode of the self-adjoint operator $D\hat{F} = 2J\partial_x^2 - 2K\cos[2(\phi^{\rm dw}(x;\phi_0,x_0) - \phi_0)]$, which explicitly reads

$$v_0(x) = \frac{\Delta}{\cosh\left((x-x_0)/\Delta\right)}. \tag{22}$$

Substituting this into (21) we find

$$\delta x_0 = \int_0^{2\pi} A_{\phi_0} d\phi_0, \quad A_{\phi_0} = \pi\Delta/2, \tag{23}$$

as it was derived in [49] with the secular perturbation theory.

A number of theoretical and experimental studies of a similar domain wall motion in liquid crystals under the influence of periodic perturbations have been performed previously [48, 50, 51, 52, 53] but the geometric nature of this effect has not been discussed. Landsberg's theory was motivated by the possibility to control wave patterns in a nonlinear media. Such a control was discussed in more detail for specific applications to nonlinear chemical reactions [54], nonlinear optics [55], hydrodynamics [56], and semiconductor microresonators [57]. Optical applications proposed by Ning and Haken were extended by Toronov and Derbov [58, 59].

Studies of special problems with a mathematical structure similar to the Lansberg-Ning-Haken formalism can be found even prior to Refs. [44, 45]. For example, the application of the rotating electric field was proposed to separate chiral molecules in a solution [60, 61]. Recently this idea was extended to a gaseous state, however, the proposed effect is expected to be observed in the non-adiabatic regime [62]. Geometric phases can also contribute to the anomalous shift of a magnetic bubble trajectory in a rotating nonuniform magnetic field (skew-deflection effect) [63].

Control over the motion of domain walls and other topological defects has been extensively studied in magnetic materials [63, 64, 65, 66]. The example of the domain wall shown above demonstrates that the projection of dynamics on the collective degrees of freedom should be performed with extra care to account for possible geometric phase effects. One can frequently find in the micromagnetics literature that equations of motion for the collective coordinates ξ read [65]

$$\mathbf{F} - \Gamma\dot{\xi} + G\dot{\xi} = 0, \tag{24}$$

where $\mathbf{F} = -\partial U/\partial\xi$ is the generalized force, Γ is the symmetric dissipation matrix, and G is the antisymmetric gyrotropic matrix. However, Eq. (24) can lead to problems. In the case of a domain wall (20), one can attempt to work with only one collective coordinate, represented by a position of the domain wall. This choice

is justified because the translation is the only continuous symmetry in the model, which should dominate all physics at low energies. However, in the model discussed, the wall was moving not because the gradient of energy was created along the wire, but rather because some parameters in the model became time-dependent. Such parameters in a static case may not induce forces on the chosen collective degrees of freedom. Thus Eq. (24) can acquire extra geometric terms in explicitly time dependent situations. As another word of caution, we note that the translational symmetries in real applications are only approximate for standard magnetic materials because of the presence of impurities and discreteness of the lattice. As discussed in [49] this presents a serious problem to achieve a pure geometric control over magnetic defects for practical applications.

4. Self-propulsion at low Reynolds numbers

One of the first applications of geometric phases in dissipative systems was proposed by Shapere and Wilczek [67, 68] to describe locomotion of microscopic organisms in a viscous fluid. This theory was based on the observation known for long time that the motion of living organisms at low Reynolds numbers is, in fact, geometrical. Microscopic living organisms propel themselves in a liquid by performing periodic changes of their shapes, leading to a rectified motion in the full phase space, that includes shapes of the body, its position and the overall orientation. One can choose a gauge in this phase space, i.e. define the rule to determine the position and the orientation angle of the body for any given shape in respect to a fixed coordinate system in the 3D-space. In such a gauge one can characterize the state of the body by a set of coordinates (x, α), where $x = (\mathbf{r}, \phi)$ is the generalized vector that describes the position and the orientation of an organism in the 3D space and α is the vector of parameters characterizing the shape of the body irrespective of x.

Body shapes are assumed directly controllable by the organism, however, being restricted, e.g. by a volume conservation, only finite and quasi-periodic changes of α can be allowed. The body interacts with the high viscosity liquid, which is described by the noncompressible Navier-Stokes equation. This equation should be solved together with the no-slip boundary conditions at the surface of the organism to guarantee the absence of an overall force and a torque on it. Since no-slip conditions are automatically satisfied for a non-moving body, for slow changes of shapes they depend only on first order time-derivatives of body coordinates. Eliminating the liquid degrees of freedom by solving the Navier-Stokes equation, the boundary conditions lead to the equation that connects changes of x and α,

$$dx = \mathbf{A}(\alpha) \cdot d\alpha, \tag{25}$$

where the connection $\mathbf{A}$ is defined on a space of body shapes. Integration over a closed path $\mathbf{c}$ in the space of body shapes leads to a purely geometric result $\delta x = \oint_{\mathbf{c}} \mathbf{A}(\alpha) \cdot d\alpha$.

The geometric theory of locomotion at low Reynolds numbers has found numerous applications, and the discussion of existing literature would be impossible in our review. Fortunately, fairly good introductions and reviews are already available [69, 70, 71]. Here we only mention that the theory was applied to determine optimal protocols for cell body changes [72, 73, 74, 75, 76]. This study determined that such optimal moves are similar to those of some living organisms [72, 75]. Discussions of simple illustrative models can be found in [73, 77]. An application of the theory to

artificially built motors to propel microscopic objects at low Reynolds numbers can be found in [78].

5. Stochastic pump

A stochastic pump is a stochastic system that responses with nonzero rectified currents to external periodic perturbations [79, 80, 81, 82, 83]. It resembles the quantum pump [84, 85, 86, 87], observed experimentally in Josephson junctions [88]. The stochastic pump effect (SPE) was observed in frequency-locked turnstile electronic devices [89, 90] and enzymatic reactions [91]. Recently, it was studied experimentally in the transport through a conical nanopore, where a strong pump flux variations as a function of relative phases of applied voltage signals were found [92].

One of the simplest realizations of the stochastic pump effect (SPE) is provided by a single state exclusion interaction model, demonstrated in Fig. 6. In this model the central bin system can have either zero or only one particle inside. The bin is connected to two absorbing states from the left and from the right, with kinetic rates shown in Fig. 6. The SPE in this model has been studied in great detail [93, 94, 95, 96, 97]. Due to the simplicity of the kinetic scheme in Fig. 6, not only average currents but also their fluctuations can be studied analytically [95].

Figure 6. A simple system demonstrating the SPE.

The model in Fig. 6 can describe the charge transport through a quantum dot in the Coulomb blockade regime [98]. Another example is the Michaelis-Menten-like enzymatic mechanism [99] realized as a following chemical reaction

$$E + S \underset{k_{-1}}{\overset{k_1}{\rightleftharpoons}} ES \underset{k_{-2}}{\overset{k_2}{\rightleftharpoons}} E + P, \tag{26}$$

where S and P are called substrate and product, and E is an enzyme molecule. An unstable complex ES gets created by either S or P binding to the enzyme, and then it dissociates back into E and S or into E and P. The model in Fig. 6 corresponds to the case of a single enzyme in the sea of macroscopic number of substrate and product molecules [95].

We consider *the moments generating function* (MGF) for the random number of transitions, n, in time T from ES into $E + P$, defined as

$$Z(\chi, T) \equiv e^{S(\chi,T)} = \sum_{n=-\infty}^{+\infty} P_n(T) e^{in\chi}, \tag{27}$$

where P_n is the probability of the event that by time T there will be n new product molecules created, counting the opposite process with the minus sign. $S(\chi, T)$ is *the cumulants generating function*, which determines all cumulants of the $S \to P$ particle flux, e.g.

$$\langle n \rangle = (-i) \left. \frac{\partial S(\chi)}{\partial \chi} \right|_{\chi=0}, \quad \mathrm{var}(n) = (-i)^2 \left. \frac{\partial^2 S(\chi)}{\partial \chi^2} \right|_{\chi=0}. \tag{28}$$

The evolution equation for the generating function $Z(\chi)$ can be derived along the following steps. It is convenient to introduce supplementary generating functions

$U_E = \sum_{n=-\infty}^{\infty} P_{nE} e^{in\chi}$ and $U_{SE} = \sum_{n=-\infty}^{\infty} P_{nSE} e^{in\chi}$, where P_{nE} is the probability that at a given time the number of generated product molecules is n and the enzyme is in the unbound state. Respectively, P_{nSE} is the probability that the enzyme is bound into the SE-complex while the number of product molecules generated is again equal to n. The master equation in such a case reads

$$\begin{aligned} \tfrac{d}{dt} P_{nE} &= -(k_1 + k_{-2}) P_{nE} + k_{-1} P_{nSE} + k_2 P_{(n-1)SE}, \\ \tfrac{d}{dt} P_{nSE} &= -(k_{-1} + k_2) P_{nSE} + k_1 P_{nE} + k_{-2} P_{(n+1)E}. \end{aligned} \tag{29}$$

Multiplying (29) by $e^{i\chi n}$ and summing over n we find

$$\frac{d}{dt} \begin{pmatrix} U_E \\ U_{SE} \end{pmatrix} = \hat{H}(\chi, t) \begin{pmatrix} U_E \\ U_{SE} \end{pmatrix}, \tag{30}$$

where

$$\hat{H}(\chi, t) = \begin{pmatrix} -k_1 - k_{-2} & k_{-1} + k_2 e^{i\chi} \\ k_1 + k_{-2} e^{-i\chi} & -k_{-1} - k_2 \end{pmatrix}. \tag{31}$$

If we set $n = 0$ at an initial moment $t = 0$, then initial conditions for (30) are $U_E(t = 0) = p_E(0)$, and $U_{SE}(t = 0) = p_{SE}(0)$, where $p_E(0)$ and $p_{SE}(0)$ are probabilities that the enzyme is respectively free or in the substrate-enzyme complex. Also, note that $Z(\chi, t) = U_E(\chi, t) + U_{SE}(\chi, t)$. The formal solution for the MGF (27) thus can be expressed as the following average of the evolution operator

$$Z(\chi, t) = \langle 1 | \hat{T} \left(e^{\int_0^t \hat{H}(\chi, t) dt} \right) | p(0) \rangle, \tag{32}$$

where $\langle 1| = (1, 1)$, and $|p(0)\rangle = (p_E(0), p_{SE}(0))$ is the vector of initial probabilities of enzyme states, and $\hat{T}$ is the time-ordering operator.

Steps leading to the adiabatic approximation for (32) can be found in [95], however, after the general discussion in Section II, it becomes clear that the generating function for a cyclic evolution of parameters becomes an exponent of the sum of two terms: geometric and dynamic ones,

$$Z(\chi) = e^{S_{\text{geom}}(\chi) + S_{\text{dyn}}(\chi)}, \tag{33}$$

$$S_{\text{geom}} = -\oint_{\mathbf{c}} \mathbf{A} \cdot d\mathbf{k}, \;\; A_m = \langle u_0(\mathbf{k}) | \partial_{k_m} | u_0(\mathbf{k}) \rangle, \tag{34}$$

$$S_{\text{dyn}} = \int_0^{T_0} dt \varepsilon_0(\chi, t) = -\frac{1}{2} \int_0^{T_0} dt \left[K - \sqrt{K^2 + 4(\kappa_+ e_\chi + \kappa_- e_{-\chi})} \right], \tag{35}$$

where $\varepsilon_0(\chi)$ is the instantaneous eigenvalue of $\hat{H}(\chi, t)$ with the larger real part, and $|u_0(\mathbf{k})\rangle$ is the corresponding eigenvector, $\mathbf{k}$ is the vector of kinetic rates in Fig. 6, $\mathbf{c}$ is the contour in this parameter space of kinetic rates, T_0 is the period of the cycle, $K \equiv \sum_m k_m$, $\kappa_\pm = k_{\pm 1} k_{\pm 2}$, $m = -2, -1, 1, 2$, and $e_{\pm\chi} = e^{\pm i\chi} - 1$.

One can trace the origin of the geometric contribution (34) to the geometric phases induced by the $SL(2, R)$ evolution [36]. If parameters k_1 and k_{-2} are time dependent, while k_2 and k_{-1} are constants, then

$$\oint_{\mathbf{c}} \mathbf{A} \cdot d\mathbf{k} = \int\int_{\mathbf{s_c}} dk_1 dk_{-2} F_{k_1, k_{-2}}, \tag{36}$$

where

$$F_{k_1, k_{-2}} = \langle \frac{\partial u}{\partial k_1} | \frac{\partial u}{\partial k_{-2}} \rangle - \langle \frac{\partial u}{\partial k_{-2}} | \frac{\partial u}{\partial k_1} \rangle. \tag{37}$$

$F_{k_1,k_{-2}}$ is the analog of the Berry curvature in quantum mechanics. Finding the eigenvectors of the Hamiltonian (31) one can derive explicitly [95]:

$$F_{k_1,k_{-2}} = \frac{e_{-\chi}(e^{i\chi}k_2 + k_{-1})}{[4\kappa_+ e_\chi + 4\kappa_- e_{-\chi} + K^2]^{3/2}}. \tag{38}$$

The MGF (33) contains information both about average fluxes and their fluctuations. In most applications only the average fluxes are needed. To extract them from expressions (34) and (35) one should write the cumulants generating function as a series in powers of the small parameter χ, and keep only the leading order contribution, i.e.

$$S_{\rm dyn} \approx iS^{(1)}_{\rm dyn}\chi + O(\chi^2), \quad S_{\rm geom} = i\chi \int\int_{S_c} dk_1 dk_{-2} F^{(1)}_{k_1,k_{-2}} + O(\chi^2). \tag{39}$$

Higher order in χ terms can reveal information about higher cumulants of stochastic fluxes, while the first order terms coincide with the average number of transferred particles up to the $i\chi$-prefactor.

For the one-step exclusion process in Fig. 6 such calculations lead to the mean $S \to P$ flux per unit time [95]

$$J = J_{\rm pump} + J_{\rm dyn}, \tag{40}$$

$$J_{\rm geom} = \int\int_{S_c} d^2k \frac{k_2 + k_{-1}}{T_0 K^3}, \tag{41}$$

$$J_{\rm dyn} = \int_0^T dt \frac{\kappa_+(t) - \kappa_-(t)}{T_0 K(t)}. \tag{42}$$

It turns out that the dynamic contribution to the current is just the steady state current averaged over time. Eqs. (41) and (42) show that the geometric contribution to the current has strikingly different properties from the dynamic one. In fact, it does not have an analog in a strict steady state situation because it is nonzero only if the contour encloses a finite area in the parameter space, i.e. at least two parameters should be driven with a phase shift different from 0 or π. Another interesting property is that this contribution reverses the sign when changing the direction of motion along the contour.

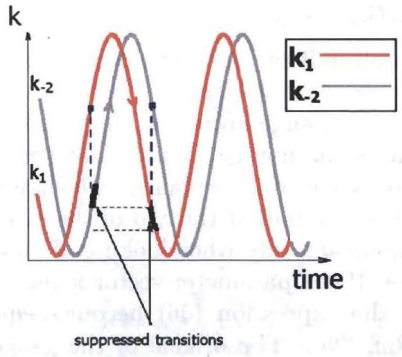

Figure 7. Illustration of the shielding mechanism of the SPE.

The phenomenon of $J_{\rm geom} \neq 0$ can be explained in simple terms, illustrated in Fig. 7. Since a molecule spends a finite time bound to the enzyme, the values of

k_1 and k_{-2} cannot influence the system during the mean unbinding time following a binding event. If the left binding rate is higher than the right one during the upramp of the cycle, then k_1 "shields" growing values of k_{-2} from having an effect, while k_{-2} shields decreasing values of k_1 during the downramp. This leads to a phase-dependent asymmetry, which is the source of the geometric pump flux.

One can notice the relation of the geometric phase (34) and the formalism of Landsberg-Ning-Haken, discussed in Section III. As far as only the average of the pump current is concerned, the pump current (40) can alternatively be derived directly from the Master Equation for the vector $\mathbf{p} = (p_{ES}, p_E)$ of probabilities of the enzyme (bin) states. Such equations have the form

$$\dot{\mathbf{p}} = \hat{H}(\mathbf{k}, \chi = 0)\mathbf{p}, \quad \dot{N}_{\mathrm{P}} = J(\mathbf{p}, \mathbf{k}), \tag{43}$$

where N_{P} is the average number of created product molecules, and $J(\mathbf{p}, \mathbf{k}) = p_{SE}k_2 - p_E k_{-2}$ is the current. This set of equations has the form (14), namely, probabilities relax to a unique steady state values at given rate constants $\mathbf{k}$, independently of the additional equation for N_{P}. The geometric phase (34), however, is more general because it contains the full information about stochastic evolution, including geometric contributions to higher cumulants. The full counting statistics of currents was measured in nanoscale electronic circuits [100]. Moreover, various stochastic effects, such as stochastic over-barrier transitions are influenced by the higher cumulants of particle fluxes [101, 102], so that the full stochastic treatment of such processes, beyond the formalism of Eqs. (43) becomes inevitable, and the geometric contribution to higher cumulants can lead to important consequences in the theory of such effects.

The quantum mechanical Berry phase allows extensions to a noncyclic evolution [104, 105]. Sinitsyn and Nemenman [106] showed that the MGF of the form (32) can be partitioned to geometric and dynamic parts even if parameters change along an open circuit.

$$Z(\chi) = e^{S_{\mathrm{geom}}(\chi) + S_{\mathrm{dyn}}(\chi)}, \tag{44}$$

where $S_{\mathrm{dyn}} = \int_0^T dt \varepsilon_0(\chi, t)$ is the quasi-stationary part of the generating function averaged over time, and

$$S_{\mathrm{geom}} = \int_{\mathbf{c}} [\mathbf{P}(\mathbf{k}) - \mathbf{A}(\mathbf{k})] \cdot d\mathbf{k}, \tag{45}$$

$$\mathbf{P} = \partial_{\mathbf{k}} \ln\langle 1|u_0\rangle, \quad \mathbf{A}(\mathbf{k}) = \langle u_0|\partial_{\mathbf{k}} u_0\rangle. \tag{46}$$

where $\langle 1| = (1, 1)$ is the vector with all unit entries. The noncyclic geometric phase contribution has no analog in a strict steady state regime. Unlike a cyclic evolution of parameters, the term $-\int_{\mathbf{c}} \mathbf{A}(\mathbf{k}) \cdot d\mathbf{k}$ is not gauge invariant. However, the integral over the additional vector $\mathbf{P}$ exactly cancels the non-gauge-invariant part of the contour integral of $\mathbf{A}$. This vector introduces the unique gauge, which follows from the averaging over the final states of the bin-system at the end of the evolution.

Since $\mathbf{P}$ is a pure gauge, it is important only when looking at an evolution along an open path in the parameter space. If the parameter vector $\mathbf{k}$ returns to its initial value at the end of the evolution, the expression (46) becomes equivalent to the cyclic geometric phase defined in Ref. [95]. The origine of the gauge invariance of the expression (45) can be traced to the Markovian property of the process. Given a state of the system at some time point, the currents counted after this point should be independent of the currents counted prior to this moment, but including previously passed currents in the MGF is equivalent to the gauge transformation $Z(\chi) \to Z(\chi)e^{S_{\mathrm{prior}}(\chi)}$.

6. Elimination of fast variables in stochastic processes

This section is technically more involved than the rest of the review, and can be safely omited by a reader not interested in mathematical details. It introduces to the method of the stochastic path integral which is a powerful technique to investigate stochastic fluxes in mesoscopic interacting systems. The approach discussed in previous section relates the derivation of the counting statistics to finding eigenvalues and eigenvectors of a non-Hermitian Hamiltonian. Such a streightforward approach becomes extremely complicated when dealing with complex systems with a mesoscopically large phase space. In many important situations stochastic path integral technique allows to make controllable approximations to derive the MGFs of fluxes even in many-body interacting mesoscopic stochastic systems. Sinitsyn and Nemenman [96] demonstrated how this technique can be applied to study geometric phases that appear in a responce to a periodic driving. In this section we discuss yet another application of geometric phases and the stochastic path integral to the problem of coarse graining stochastic kinetics.

Berry phases often appear in quantum mechanical applications when one attempts to eliminate fast degrees of freedom and reduce a problem to an effective one which includes only slow variables. Such an approach is known as the Born-Oppenheimer approximation. This approximation was very successful for describing near-equilibrium properties of most molecules. According to it, initially one solves a much simpler Schrödinger equation for electrons, treating nuclear degrees of freedom as adiabatically slowly changing parameters. After this, one assumes that the nuclei move on a single potential-energy surface created by the faster moving electrons. An interesting ingredient in this approach was the observation that geometric phases, acquired by electrons in a potential of slowly moving nuclei, influence the dynamics of slow degrees of freedom [14, 15, 107].

The evolution equations for MGFs in stochastic processes are similar to the quantum mechanical Schrödinger equation [108]. This mathematical similarity was widely employed, for example, to study the counting statistics in electronic transport [109, 110, 111], to estimate over-barrier escape probabilities [101, 102], or to classify stochastic phase transitions [112]. Many of the applications of this approach were restricted to relatively simple systems with only a few interacting species because generally quantum mechanical equations are not simpler to investigate than the stochastic ones.

Recently, a stochastic/quantum mechanical analogy was proposed to simulate the behavior of large stochastic networks of biochemical reactions, which include many different types of chemical species and chemical reactions [113]. One of the difficulties in studying such networks is their stiffness, i.e. a strong time-scale separation of various processes. In application to stochastic processes, the Born-Oppenheimer approximation rigorously captures statistical characteristics of chemical processes at coarse-grained scales.

In this section we show a simple example of how a reduction of a model can be achieved and how geometric phases influence the evolution of slow variables. For a demonstration we again consider the Michaelis-Menten type of conversion of S into P via creation of a substrate-enzyme complex, studied in previous section, however, now we assume that numbers of substrate and product molecules (N_{S} and N_{P} respectively) are independent dynamic variables, subject to all conservation laws provided by the given kinetic scheme. We also assume that kinetic rates to create the enzyme substrate

complex are proportional to the absolute numbers of substrate and product molecules N_S and N_P so that the full set of reactions reads

(i) forward substrate-enzyme complex formation, $S + E \to SE$, with rate $k_1 N_S$;

(ii) backward substrate-enzyme complex formation, $P + E \to SE$, with rate $k_{-2} N_P$;

(iii) complex backward decay, $SE \to S + E$, with rate k_{-1};

(iv) product emission $SE \to E + P$, with rate k_2.

If we have only one enzyme but $N_S, N_P \gg 1$, it takes many identical steps for enzyme to convert a substantial number of substrates into products. This creates a time-scale separation, which can be used to reduce the model to an effective process

$$S \to P. \tag{47}$$

Our goal is to find statistical characteristics of the coarse-grained reaction (47). Lets choose a time scale δt, which is much larger than a typical time of a single enzyme turnover, but much smaller than the time when substantial relative change of substrate or product amount is developed. Suppose that we are looking for the moments generating function of the number of product molecules n_P created during a relatively long time $T \gg \delta t$:

$$\mathcal{Z}(\chi_C) = e^{\mathcal{S}(\chi_C)} = \sum_{n_P=-\infty}^{\infty} P(n_P|T) e^{i n_P \chi_C}. \tag{48}$$

As it is discussed in [109, 108], if one knows the statistical properties of fluxes at time scales δt then the MGF at larger time scales can be written in the form of a stochastic path integral. We will derive the stochastic path integral representation of the MGF (48).

In previous section we already found the full counting statistics of the fluxes in Michaelis-Menten model with slowly time dependent parameters. To apply it to our model we should redefine kinetic rates as $k_1 \to k_1 N_S(t)$ and $k_{-2} \to k_{-2} N_P(t)$. This does not solve our problem completely, because at this stage we do not know explicit time dependence of $N_S(t)$ and $N_P(t)$, because now we consider them as slow but dynamic variables. However, we can discretize time into intervals $(t_k, t_k + \delta t)$ of sufficiently small durations δt, so that a relative change of the number of product molecules is small $\langle \delta n_P(t_k) \rangle / N_{P/S}(t_k) \ll 1$, but $\langle \delta n_P(t_k) \rangle \gg 1$. The probability distributions of $\delta n_P(t_k)$ are then given by the inverse Fourier transforms of the corresponding MGFs, which we found in previous section:

$$P(\delta n_P(t_k)) = \frac{1}{2\pi} \int_{-\pi}^{\pi} d\chi(t_k) e^{-i\chi(t_k)\delta n_P(t_k) + S_{MM}(\chi(t_k); N_S(t_k), N_P(t_k), \delta t)}, \tag{49}$$

where $S_{MM} = S_{geom} + S_{dyn}$ is the same as in (44) during time δt.

The MGF of the created number of product molecules during a large time interval $(0, T)$ is given by the sum over all possible paths in the parameter space, weighted by probabilities (49) and by delta-functions, responsible for the conservation laws. Using that $n_P = \sum_{k=1}^{T/\delta t} \delta n_P(t_k)$, the MGF of this number is

$$Z(\chi_C) \equiv \langle e^{i\chi_C n_P} \rangle = \prod_k \int dN_S(t_k) dN_P(t_k) \int d(\delta n_P(t_k)) P[\delta n_P(t_k)] e^{i\chi_C \delta n_P(t_k)} \times$$
$$\delta(N_S(t_{k+1}) - N_S(t_k) + \delta n_P(t_k)) \delta(N_P(t_{k+1}) - N_P(t_k) - \delta n_P(t_k)). \tag{50}$$

where δ-functions take care of conservation laws. We rewrite them as integrals over oscillating exponents

$$\delta(N_{\rm S/P}(t_{k+1}) - N_{\rm S/P}(t_k) \pm \delta n_{\rm P}(t_k)) = \\ \frac{1}{2\pi}\int_{-\pi}^{+\pi} d\chi_{\rm S/P}(t_k) e^{i\chi_{\rm S/P}(t_k)[N_{\rm S/P}(t_{k+1}) - N_{\rm S/P}(t_k) \pm \delta n_{\rm P}(t_k)]} \tag{51}$$

and substitute (51) and (49) into (50). After this, integrals over $\delta n_{\rm P}(t_k)$ produce new δ-functions, which are easily removed by integration over $\chi(t_k)$, leaving us only with a path integral over slow $N_{\rm S/P}(t_k)$ and $\chi_{\rm S/P}(t_k)$ variables. Taking a continuous limit $f(t_{k+1}) - f(t_k) \to \dot{f}(t)dt$, we can rewrite the MGF as a path integral over slow variables only,

$$\langle e^{i\chi_C n_{\rm P}} \rangle = \int DN_{\rm S}(t) \int DN_{\rm P}(t) \int D\chi_{\rm S}(t) \int D\chi_{\rm P}(t) e^{S(\chi_{\rm C}, T)}, \tag{52}$$

where $S(\chi_{\rm C}, T)$ can be partitioned into a "classical" and geometric parts

$$S(\chi_{\rm C}, T) = S^{\rm cl}(\chi_{\rm C}, T) + S^{\rm geom}(\chi_{\rm C}, T), \tag{53}$$

such that

$$S^{\rm geom}(\chi_{\rm C}, T) = -\int_{\mathbf{c}} [A_{N_{\rm S}} dN_{\rm S} + A_{N_{\rm P}} dN_{\rm P} + A_{\chi_{\rm S}} d\chi_{\rm S} + A_{\chi_{\rm P}} d\chi_{\rm P}], \tag{54}$$

$$A_x = \langle u_0(\chi_{\rm S} - \chi_{\rm P} + \chi_C) | \partial_x | u_0(\chi_{\rm S} - \chi_{\rm P} + \chi_{\rm C}) \rangle, \tag{55}$$

$$S^{\rm cl}(\chi_{\rm C}, T) = \int_0^T dt\, [i\chi_{\rm S}\dot{N}_{\rm S} + i\chi_{\rm P}\dot{N}_{\rm P} + H_{\rm MM}(N_{\rm S}, N_p, \chi_{\rm S} - \chi_{\rm P} + \chi_{\rm C}). \tag{56}$$

where $\mathbf{c}$ is the contour of the trajectory in the slow parameter space, x belongs to the set $\{N_{\rm S}, N_{\rm P}, \chi_{\rm S}, \chi_{\rm P}\}$ and $H_{\rm MM}$ plays the role of the effective Hamiltonian

$$H_{\rm MM} = \frac{1}{2}\left(K - \sqrt{K^2 + 4[N_{\rm S} k_1 k_2 (e^{i(\chi_{\rm S} - \chi_{\rm P} + \chi_{\rm C})} - 1) + N_{\rm P} k_{-1} k_{-2} (e^{-i(\chi_{\rm S} - \chi_{\rm P} + \chi_{\rm C})} - 1)]}\right), \tag{57}$$

where $K \equiv k_1 N_{\rm S} + k_{-2} N_{\rm P} + k_{-1} + k_2$. This Hamiltonian is different from what one would expect if the conversion of S into P were a Poisson process, which reflects the non-Poisson nature of enzyme mediated fluxes. The geometric part of the action (54) is the result of the pump fluxes.

The path integral representation (52) is the formal solution of the problem of removal of fast degrees of freedom in the sense that it expresses the needed MGF in terms of only slow variables $N_{\rm S}, N_{\rm P}, \chi_{\rm S}, \chi_{\rm P}$ and does not depend on "bound/unbound" degrees of freedom of the enzyme.

Since average numbers $\langle N_{\rm S} \rangle$ and $\langle N_{\rm P} \rangle$ are assumed large, one can use the saddle point solution of the path integral to derive semiclassical equations of motion for slow variables. Varying the action results in four coupled differential equations

$$\begin{aligned} i\dot{N}_{\rm S} &= -\tfrac{\partial H_{\rm MM}}{\partial \chi_{\rm S}} - iF_{\chi_{\rm S}, N_{\rm S}} \dot{N}_{\rm S} - iF_{\chi_{\rm S} N_{\rm P}} \dot{N}_{\rm P}, \\ i\dot{N}_{\rm P} &= -\tfrac{\partial H_{\rm MM}}{\partial \chi_{\rm P}} + iF_{\chi_{\rm S}, N_{\rm S}} \dot{N}_{\rm S} + iF_{\chi_{\rm S} N_{\rm P}} \dot{N}_{\rm P}, \\ i\dot{\chi}_{\rm S} &= \tfrac{\partial H_{\rm MM}}{\partial N_{\rm S}} + iF_{\chi_{\rm S}, N_{\rm S}} \dot{\chi}_{\rm S} + iF_{\chi_{\rm S} N_{\rm P}} \dot{\chi}_{\rm P} + iF_{N_{\rm S}, N_{\rm P}} \dot{N}_{\rm P}, \\ i\dot{\chi}_{\rm P} &= \tfrac{\partial H_{\rm MM}}{\partial N_{\rm P}} - iF_{\chi_{\rm S}, N_{\rm S}} \dot{\chi}_{\rm S} - iF_{\chi_{\rm S} N_{\rm P}} \dot{\chi}_{\rm P} - iF_{N_{\rm S}, N_{\rm P}} \dot{N}_{\rm S}, \end{aligned} \tag{58}$$

where $F_{x_1,x_2} = -i(\partial A_{x_2}/\partial x_1 - \partial A_{x_1}/\partial x_2)$ and we used that A_{x_m} depends on χ_S, χ_P via the combination $(\chi_S - \chi_P)$ which leads to the relations $F_{\chi_n,\chi_m} = 0$, $F_{\chi_S,N_S} = -F_{\chi_P,N_S}$ and $F_{\chi_S,N_P} = -F_{\chi_P,N_P}$. As it is discussed in [109] the boundary conditions are given by initial values of $N_{S/P}(0)$ and by $\chi_{S/P}(T) = 0$.

For $\chi_C = 0$ there is a solution of equations (58), such that $\chi_S = \chi_P = 0$ and N_S, N_P satisfy coupled equations, which are known to coincide with the mean field equations

$$\begin{aligned} i\dot{N}_S &= -i\Omega_{\chi_S,N_S}\dot{N}_S - i\Omega_{\chi_S N_P}\dot{N}_P - \tfrac{\partial H_{MM}}{\partial \chi_S}|_{\chi_S=\chi_P=\chi_C=0}, \\ i\dot{N}_P &= i\Omega_{\chi_S,N_P}\dot{N}_S + i\Omega_{\chi_S N_P}\dot{N}_P - \tfrac{\partial H_{MM}}{\partial \chi_P}|_{\chi_S=\chi_P=\chi_C=0}, \end{aligned} \tag{59}$$

where $\Omega_{x_1,x_2} = F_{x_1,x_2}|_{\chi_S=\chi_P=\chi_C=0}$. Explicitly, for our model one can find that

$$\begin{aligned} \Omega_{\chi_S,N_S} &= k_1(k_2+k_{-1})\tfrac{(k_2+k_{-2}N_P)}{K^3}, \\ \Omega_{\chi_S,N_P} &= k_{-2}(k_2+k_{-1})\tfrac{(k_2+k_{-2}N_P)}{K^3}. \end{aligned} \tag{60}$$

If substrate and product do not have other dynamics but the conversion into each other via the ES complex, then $\dot{N}_P = -\dot{N}_S$, $\frac{\partial H_{MM}}{\partial \chi_S}|_{\chi_S=\chi_P=\chi_C=0} = -\frac{\partial H_{MM}}{\partial \chi_P}|_{\chi_S=\chi_P=\chi_C=0} = i(k_1k_2N_S - k_{-1}k_{-2}N_P)/K$, and the evolution of N_P, according to (59) reads

$$\dot{N}_P = \frac{(k_1k_2N_S - k_{-1}k_{-2}N_P)}{K} + (k_2+k_{-1})\frac{(k_1\dot{N}_S + k_{-2}\dot{N}_P)(k_2+k_{-2}N_P)}{K^3}. \tag{61}$$

The first term in (61) is just the usual quasi-steady-state prediction, and the second term is a correction due to the geometric phase contribution to the effective action. We note again that Eqs. (58) contain information both about average fluxes and their fluctuations, while the result (61) is equivalent to the mean-field prediction for the average number of N_P. Substituting solution of (58) into (53) one can find the full counting statistics of created product molecules n_P.

Terms similar to the geometric phase corrections in (58) naturally appear also in the variational approaches to chemical kinetics [114]. Generally, the geometric phase correction in (61) is smaller than the quasi-steady state part. However, there are situations when it can be important due to its specific symmetries [106]. Equations of motion, such as (58) have been known in condensed matter physics, where similar Berry phase terms lead to distinct effects, such as the anomalous and the spin Hall effects [6, 7, 8].

7. Driven limit cycle

An interesting geometric phase was found by Kagan *et al* [115] in dissipative systems evolving to a limit cycle. In addition to a geometric phase that appears after the elimination of quickly decaying modes, they found also a geometric phase which originates from the nontrivial topology of the limit cycle itself. Consider the following evolution equation

$$\frac{d\phi}{dt} = \Omega(\phi,\mu), \tag{62}$$

where $\Omega(\phi) = \Omega(\phi+2\pi)$ is the instantaneous frequency and μ is the vector of internal parameters, which is slowly and periodically time-dependent. Since the evolution is

periodic we can call ϕ a phase and can identify states with ϕ different by an integer times 2π. Introducing another variable

$$\theta(\phi,\mu) = \int_0^{\phi} \frac{\omega(\mu)}{\Omega(\phi',\mu)} d\phi', \tag{63}$$

where

$$\omega(\mu) = \left(\frac{1}{2\pi} \int_0^{2\pi} \frac{1}{\Omega(\phi',\mu)} d\phi' \right)^{-1}, \tag{64}$$

Kagan *et al* showed that for adiabatic cyclic evolution of μ the phase (63) becomes the sum of a dynamic and a geometric parts,

$$\theta(T) = \theta_{\rm dyn}(T) + \theta_{\rm geom}(T), \tag{65}$$

where T is a period of the adiabatic evolution of parameters,

$$\theta_{\rm dyn}(T) = \int_0^T dt \omega(\mu(t)), \tag{66}$$

and

$$\theta_{\rm geom}(T) = \oint \mathbf{A} \cdot d\mu, \tag{67}$$

where

$$\mathbf{A} = \int_0^{2\pi} \frac{d\phi}{2\pi} \left[\frac{\omega(\mu(t))}{\Omega(\phi,\mu)} \partial_\mu \theta(\phi,\mu)) \right]. \tag{68}$$

One can look at the geometric phase (67) from the point of view of the stochastic path integral representation, discussed in the previous section. Similarly to the derivation of the stochastic path integral one can promote the evolution (62) to a Hamiltonian one by introducing a variable Λ, which is canonically conjugated to ϕ with the Hamiltonian

$$H(\Lambda,\phi) = \Lambda\Omega(\phi,\mu). \tag{69}$$

The phase evolution (62) then follows from canonical equations, i.e.

$$\frac{d\phi}{dt} = \frac{\partial H}{\partial \Lambda}. \tag{70}$$

Sinitsyn and Ohkubo [116] showed that in such a Hamiltonian evolution $\theta_{\rm geom}$ becomes a Hannay angle [29], which is a type of geometric phases in classical mechanics, responsible e.g. for the rotation of the Foucault pendulum, and many other subtle effects.

8. Thermodynamic constraints and geometric phases

Many applications of geometric phases in stochastic kinetics can be found in systems driven close to the thermodynamic equilibrium. Examples can be found among molecular motors or mesoscopic electronic circuits when studying their response to periodic external perturbations. Before applying of a time-dependent driving, such structures usually are at the thermodynamic equilibrium with their environment. Thermodynamic laws impose additional constraints on the kinetic rates. Such constraints guarantee that the Boltzmann distribution at given temperature will describe the equilibrium state.

What are the consequences of such constraints for geometric phases? One useful observation is that the steady state at the thermodynamic equilibrium does not support any current on average, unless there are external fields in the system, such as the magnetic field, which explicitly break the time-reversal symmetry. In systems with detailed balance, a strict quasi-steady state approximation predicts exactly zero fluxes in response to adiabatically slow perturbations. The geometric phase is the only mechanism that can be responsible for a nonzero current in such slowly driven systems, and hence it should play an important role close to the thermodynamic equilibrium. In this section we discuss several examples in support of this conclusion.

8.1. Reversible ratchet

A simple example of a device working near the thermodynamic equilibrium is called the reversible ratchet. It is a system of particles diffusing in a periodic in space potential $V(x,t) = V(x+L,t)$. The particle distribution $\rho(x,t)$ satisfies the Fokker-Plank equation, predicting that for a fixed potential profile, $\rho(x,t)$ relaxes to the Boltzmann distribution $\rho(x) = Ce^{-V(x)/k_BT}$, where C is a normalization constant.

Now, assume that the shape of the potential changes periodically and slowly with time, with some period T, as it is shown in Fig. 8. Currents in a discrete version of this model were studied by Markin and Astumian [117]. The continuous model was studied by Parrondo in [118], who derived the explicit expression for the current of particles in such a system in the limit of adiabatically slow changes of the potential. The paradox is that for adiabatically slow changes, one can expect that the particle distribution would have enough time to relax to an instantaneous equilibrium distribution, i.e. it is expected to have a form $\rho(x,t) \approx C(t)e^{-V(x,t)/k_BT}$. Such a varying Boltzmann distribution does not predict any current on average in the system at any moment of time, while apparently the solution of the problem predicts a finite current.

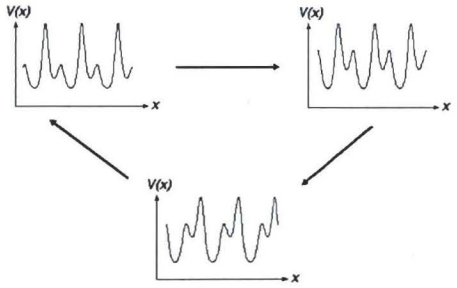

Figure 8. Snapshots of a reversible ratchet potential at three stages of its evolution.

Sinitsyn and Nemenman [96] explored this model from the point of view of the stochastic path integral representation of the current MGF $Z(\chi)$. They showed that

$$Z(\chi,T) = e^{i\chi \oint_{\mathbf{c}} \mathbf{A}(\mathbf{k})\cdot d\mathbf{k} + O(\chi^2)}, \tag{71}$$

where $\mathbf{k}$ is the vector of parameters controlling the shape of $V(x)$, and $\mathbf{c}$ is the contour in this parameter space. According to (71) the geometric phase is not zero, and contributes to the linear order in the counting parameter χ of the MGF. Moreover, there is no contribution to this order from the quasi-stationary term. This result confirms that a nonzero current in an adiabatic reversible ratchet is finite, and this

current is purely geometrical. It can be totally controlled by choosing a proper contour in the space of potential shapes.

An interesting observation about this effect was also made by Shi and Niu [119], who showed that this current can be quantized, and this quantization can be related to the Chern number of a Bloch band related to the solutions of the Fokker-Plank equation in a periodic potential.

8.2. Geometric phases and fluctuation-dissipation relations.

The adiabatic SPE appears when two time-dependent periodic perturbations are applied. We showed that the average flux of the "charge" of type A pumped after an infinitesimal cyclic driving of external fields $h_B(t)$ and $h_C(t)$, is proportional to the area inside the driving contour. Also we showed that the pumped current reverses its sign when a system is driven along the same contour but in the opposite direction. This situation can be expressed as the following law.

$$\delta q_A = F^A_{BC} dh_B \wedge dh_C, \tag{72}$$

where δq_A is a total flux of A that on average passes through a system during one cycle of the adiabatic periodic evolution, $dh_B \wedge dh_C$ is the infinitesimal area, inclosed by the contour in the control parameter space and F^A_{BC} is the proportionality coefficient.

It is well established that near the thermodyanamic equilibrium some transport coefficients can be expressed through correlation functions at the equilibrium, as it is stated by the Fluctuation-Dissipation Theorem [120]. What such relations can tell about the coefficient F^A_{BC}? The quantum version of the adiabatic pump effect can be calculated using the Kubo formula approach [86]. One can derive the analogous result for a classical stochastic pump, operating near the thermodynamic equilibrium, using a classical version of the linear response theory [121].

Assume that variables B and C, coupled to the fields h_B and h_C are time reversal invariant. This means that at the thermodynamic equilibrium with fixed h_B and h_C all currents are zero on average

$$\langle J_A(t) \rangle_{h_B, h_C} = 0, \tag{73}$$

where $\langle \ldots \rangle_{h_B h_C}$ means the average over the equilibrium distribution at given values of h_B and h_C. We start at such an equilibrium state and increase h_B, h_C by small amounts δh_B and δh_C such that $h_\alpha(t) = h_\alpha(0) + \delta h_\alpha \theta(t)$, where $\alpha = A, B$. According to the linear response theory the current of A at a moment $t > 0$ reads

$$J_A(t) = \delta J_{AB}(t) + \delta J_{AC}(t), \tag{74}$$

where

$$\delta J_{A,\alpha}(t) = 2i \int_0^t dt' \chi''_{J_A,\alpha}(t - t') \delta h_\alpha, \tag{75}$$

and $\chi''_{J_A,\alpha}(\omega)$ is the response function [120]. Let $\chi''_{J_A,\alpha}(\omega)$ be the Fourier transform of $\chi''_{J_A,\alpha}(t)$, then

$$\delta J_{A,\alpha}(t) = 2i \int_0^t dt' \int \frac{d\omega}{2\pi} \chi''_{J_A,\alpha}(\omega) e^{i\omega(t-t')} \delta h_\alpha = \int \frac{d\omega}{2\pi} \frac{2\delta h_\alpha \chi''_{J_A,\alpha}(\omega)}{\omega} e^{i\omega t}, \tag{76}$$

where we used that J_A and B or C have different time reversal properties so that the static suseptibility [120] is identically zero, i.e.

$$\int \frac{d\omega}{2\pi} \frac{\chi''_{J_A,\alpha}(\omega)}{\omega} = 0. \tag{77}$$

The classical Fluctuation-Dissipation Theorem [120] states that

$$\chi''_{J_A,\alpha}(\omega) = \frac{\beta\omega}{2} S_{J_A\alpha}(\omega), \quad \beta = 1/k_{\rm B}T, \tag{78}$$

where $S_{J_A,\alpha}(\omega)$ is the Fourier transform of the correlator at the equilibrium.

$$S_{J_A\alpha}(t-t') = \langle J_A(t)\alpha(t')\rangle, \quad \alpha = B, C. \tag{79}$$

Substituting (78) and (79) into (76) and integrating over time, the total flux of A passed due to such a small step perturbation reads

$$\delta q_A = Q_{AB}\delta h_B + Q_{AC}\delta h_C, \tag{80}$$

where

$$Q_{AB} = \beta \int_0^\infty dt S_{J_A B}(t), \tag{81}$$

$$Q_{AC} = \beta \int_0^\infty dt S_{J_A C}(t). \tag{82}$$

Note that both Q_{AB} and Q_{AC} are completely determined by the equilibrium correlation functions at nonzero B and C. Imagine that the adiabatic evolution in the control parameter space consists of such small steps, then after one cycle the total transferred charge is

$$\delta q_A = \oint_{\mathbf{c}} \{Q_{AB} dh_B + Q_{AC} dh_C\} = \int\int_{\mathbf{S_c}} dh_B \wedge dh_C F^A_{BC}, \tag{83}$$

where $\mathbf{c}$ is the contour in the parameter space and F^A_{BC} is the transport coefficient, that we have been looking for. According to the Stokes theorem

$$F^A_{BC}(h_B, h_C) = \frac{\partial Q_{AC}}{\partial h_B} - \frac{\partial Q_{AB}}{\partial h_C}. \tag{84}$$

Eq. (84) shows that the pump transport coefficient can be expressed as a circulation of some vector $\mathbf{Q}$ in space of controlled parameters h_B and h_C, which components are correlators (81,82) at equilibrium. Such relations indicate that the ability of a system to perform as a stochastic pump in response to periodic perturbations can, in principle, be inferred from properties of the system in the thermodynamic equilibrium. This can lead to simplifications during numerical or perturbative analysis of molecular motor operations, because the equilibrium properties are relatively easy to investigate. For example, simulations of free energy landscapes are achievable for complex biological molecules such as a kinesine molecular motor [103].

8.3. Beyond adiabatic and perturbative limits

So far we discussed the effect of detailed balance constraints on systems driven adiabatically slowly. Quantum mechanical Berry phase can be generalized to a non-adiabatic evolution [104]. Following this analogy Ohkubo showed that geometric phases in the stochastic kinetics also can be considered in the non-adiabatic regime [94].

Recently, a number of exact results in the theory of stochastic pump effect were derived, which are valid in nonperturbative and nonadiabatic regimes [122, 123]. These results were motivated partly by recent experiments with catenane molecules [124, 125, 126]. Such molecules are made of coupled rings as in Fig. 9. By changing

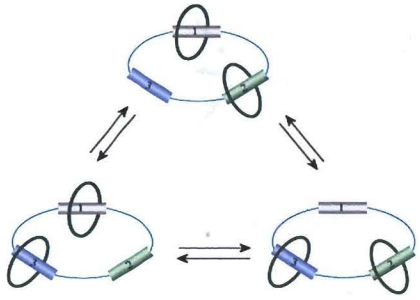

Figure 9. Three metastable states of a catenane molecule.

external conditions periodically, one can modulate affinities of special sites on a larger ring and force the smaller ones to perform rotating motion around it. Astumian in [127] showed that for a 2-ring system, the adiabatic modulation of affinities alone is insufficient to perform a preferred rotation of one ring around another on average, while for a 3-ring molecule shown in Fig. 9 such a control is allowed. Rahav, Horowitz and Jarzynski [122] showed that this result is a consequence of a much more general "no-pumping" theorem. They showed that for a periodic *non-adiabatic* driving protocol the average flux Q passed through any link $i-j$ of a graph representing a finite Markov chain can be written as a sum of a geometric and a dynamic parts, i.e.

$$Q = \int_0^T dt J_{\rm dyn}(t) + \oint_{\mathbf{c}} \mathbf{A} \cdot d\mathbf{p}. \tag{85}$$

The second term in (85) is geometrical and depends only on the path $\mathbf{c}$ in the space of values of the state probability vector $\mathbf{p}$, and T is the driving period. Itself, this representation is not an explicit solution because the evolution of the probability vector $\mathbf{p}$ is not assumed to be known. However, authors of [122] showed that when the detailed balance is imposed, the dynamic part in (85) becomes identically zero, so that even for fast driving the flux becomes purely geometrical. Moreover, parametrizing kinetic rates by parameters E_i and $W_{ij} = W_{ji}$ such that $k_{ji} = k \exp[E_i - W_{ij}]$ they showed that the connection $\mathbf{A}$ is the function of only "barrier heights" W_{ij} but not of "well depths" E_i. As a consequence, if only several well depths E_i are varied, while W_{ij} remain fixed, and if the probability vector returns to the initial values at the end of the evolution, the geometric term becomes zero because $\oint_{\mathbf{c}} \mathbf{A} \cdot d\mathbf{p} = \mathbf{A} \cdot \oint_{\mathbf{c}} d\mathbf{p} = 0$, which proves the no-pumping theorem.

Chernyak and Sinitsyn [123] derived and proved even more general Pumping-Restriction Theorem (PRT), which includes the no-pumping theorem [122] as a special case. The PRT states that not all pumped fluxes on a finite Markov chain are independent. Rather they can be considered as vectors in a vector space with the dimension given by the maximum number of driven barriers W_{ij}, which removal does not break the graph into disjoined components. A trivial consequence of this theorem is that the pump currents through any link on a tree-like graph, such as the one in Fig. 10, is exactly zero. Indeed, removal of any link from a tree breaks it into disjoined

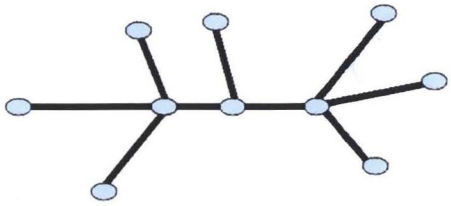

Figure 10. A graph with a tree-like topology.

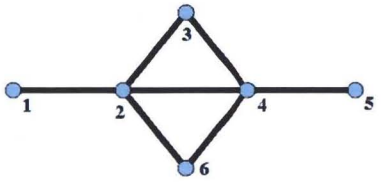

Figure 11. A six state Markov chain.

components, and according to the PRT, the pump current on such a graph should be zero.

The result for a tree graph is expected because for periodic driving any flux through any link on a tree-like graph should eventually return through the same link, so that the integrated current must be zero. However, the PRT leads to many less obvious predictions. For example, for a graph in Fig. 11, driving only the rates related to links $2-3$ and $3-4$, one can induce a finite pump current but according to the PRT, a pump current through any other link will be proportional to the pump current through the link $2-3$ with a constant proportionality coefficient. The PRT also predicts that an arbitrary periodic driving of parameters on the links $1-2$ and $4-5$ in Fig. 11 alone cannot induce the pump effect. Moreover, the second part of the PRT states that if pump currents are allowed, and if there are restrictions on their values predicted by the first part of the PRT, then these particular restrictions do not depend on parameters E_i.

Existence of exact results such as the no-pumping and the pumping-restriction theorems means that there are strong constraints that should be considered in designing nanoscale devices, interacting with environment. At this stage it is unclear whether these theorems can be extended, e.g. to include higher flux cumulants, and whether the PRT can be related to other exact results in non-equilibrium thermodynamics, such as the Jarzynski equality [128]. We note that a number of fluctuation theorems have been found for applications to ratchet systems and molecular motors [129, 130, 131, 132, 133, 134], however, their connections to geometric phases are unknown.

9. Geometric phases and molecular motors

In this section we demonstrate how geometric phases appear in the control theory of the molecular machines. Existing applications of geometric phases in mathematical robotics were motivated by the same geometric structure as the one discussed by Shapire and Wilczek in relation to the living cell locomotion [67, 68]. Indeed, like living

organisms, robots often perform important tasks having only limited possibilities to change their internal degrees of freedom. However, when interacting with environment, periodic changes in internally controlled parameters lead to a nonzero effect on the overall robot position or on its surrounding. The geometric theory of robotic motion has been widely discussed in mathematical literature, for example, see [12, 135, 136] for introduction and further references.

Many biological molecules resemble motors, and sometimes operate according to principles similar to those of the macroscopic machines used by humans. Molecular motors are ubiquitous in living organisms. They are employed, for example, for transport, injecting viruses into living cells, unzipping the DNA, and storing energy [137, 138].

The experimental progress with synthesizing and observing the motion of molecular motors is remarkable. Reviews [139, 140] describe many recently synthesized molecules such as rotaxanes and catenanes, which are able to perform a prescribed mechanical motion in response to external stimulus. Moreover, the experimental techniques to observe a molecular motion also reached a level when discrete steps in a molecular motor operation can be observed [142, 143]. Measurements of noise and even of distribution tails of reaction events statistics became feasible [141, 142, 144].

Better understanding of the working principles of nanoscale machines will provide the possibility to rebuild them in order to perform specially prescribed operations. Recently, the artificially modified F_1-subunit of the natural molecular motor F_0F_1-ATPase was shown to demonstrate a conversion of external perturbations to chemical energy [145]. One possibility to modify this molecular motor, shown in Fig. 12, was realized in [146]. In living cells, the molecular motor F_0F_1-ATPase converts energy of H^+ gradient into the chemical energy stored in ATP molecules, or acts in opposite direction to pump ions using chemical energy stored in ATP.

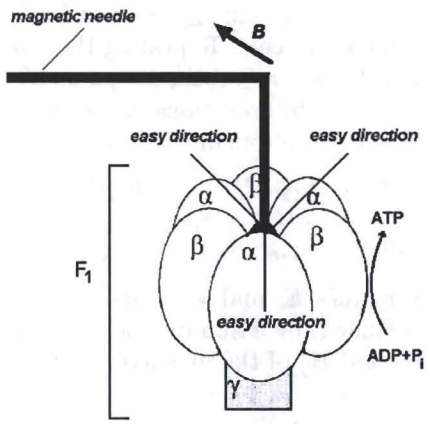

Figure 12. F_1-subunit of the natural molecular motor F_0F_1-ATPase with attached magnetic needle in external magnetic field **B**.

At molecular level, fluctuating forces are considerably stronger than typical external fields. For example, unlike fuel to drive a car, molecular motors, such as the F_0F_1-ATPase, absorb chemical energy in discrete portions and randomly. This leads to the shot noise in their operations. Molecular motors are also subjects of

considerable thermal fluctuations. All these fluctuations are not merely a theoretical complication. For example, vesicle transport via the "hitchhiking" mechanism, proposed in [147] intrinsically relies on stochasticity. In addition, single molecule experiments demonstrated that noise measurements provide important information about the molecular structure [142], and thus can be employed to uncover details of the molecular motor working cycle. The theory of molecular motor operations must include this stochasticity.

Many efforts have been applied to understand the thermodynamics of molecular motors, using the models of stochastic pumps and ratchets [80, 81, 82, 83, 148], see [149, 150, 151, 152] for reviews. However, the geometric point of view on molecular motor operations is relatively novel [95, 96, 118, 127, 153].

For a demonstration we consider a model motivated by the structure shown in Fig. 12. The molecule has an approximate 3-fold symmetry (except its rotating γ-subunit), and if the magnetic coupling to the needle is weaker than the size of the potential barrier W between any pair of metastable states, the kinetics can be minimally described by a 3-state model with some stochastic transition rates between any pair of neighboring states, as shown in Fig. 3. We assume that every transition between two states is accompanied by ADP $\rightarrow$ ATP conversion for a clockwise rotation of the γ-subunit, to which the magnetic propeller is attached, and the opposite reaction happens after a counter-clockwise rotation. Assume that this structure is placed in the external rotating magnetic field. Due to the magnetic needle, it is possible to control relative energies of 3 states and potential barriers between them by applying a rotating external magnetic field. We'll be interested in the number of full rotations of the needle and hence the attached to it γ-subunit, generated by this driving near the thermodynamic equilibrium.

One can parametrize kinetic rates of an arbitrary Markov chain with detailed balance conditions so that for any pair of sites i and j these rates are written as $k_{ij} = ke^{E_j - W_{ij}}$, where E_i is the depth of a potential well i, and $W_{ij} = W_{ji}$ is the size of the potential barrier between sites i and j. Energy scale is $k_B T = 1$, and k is a constant rate coefficient, which sets the time scale. Repeating the same steps as those leading to the MGF of fluxes through the bin in "Stochastic pump effect" section, one would find that the MGF of the number of full rotations in the clockwise direction is again given by Eq. (32) but with a new Hamiltonian that reads

$$\hat{H}(\chi) = \begin{pmatrix} -(k_{21}+k_{31}) & k_{12}e^{-i\chi/3} & k_{13}e^{i\chi/3} \\ k_{21}e^{i\chi/3} & -(k_{32}+k_{12}) & k_{23}e^{-i\chi/3} \\ k_{31}e^{-i\chi/3} & k_{32}e^{i\chi/3} & -(k_{13}+k_{23}) \end{pmatrix}. \tag{86}$$

The magnetic field modulates parameters E_i and W_{ij}, and hence k_{ij}. The 3-fold symmetry of the molecule can be included, by assuming the following dependence of these parameters on components B_x and B_y of the magnetic field.

$$\begin{aligned} E_1 &= b_y, \\ E_2 &= b_x \cos(\pi/6) - b_y \cos(\pi/3), \\ E_3 &= -b_x \cos(\pi/6) - b_y \cos(\pi/3), \end{aligned} \tag{87}$$

where $b_{x/y} = -B_{x/y}M$, and M is the magnetization of the needle. Suppose that maximums of the potential barriers are shifted from the potential minima by an angle ϕ. Thus the reasonable assumption for their dependence on the magnetic field would

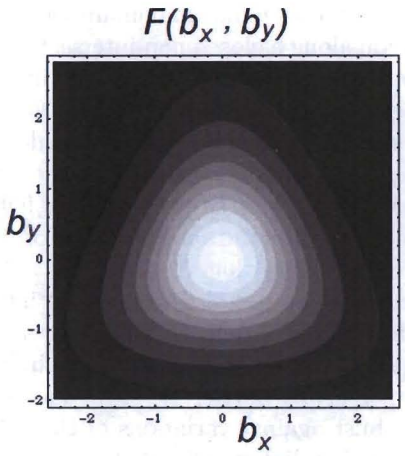

Figure 13. 3D-plot of the "Berry curvature" function $F(b_x, b_y)$ from Eq. (89), as a function of controllable parameters b_x and b_y.

be

$$\begin{aligned} W_{12} &= W + b_y \cos(\phi) + b_x \sin(\phi), \\ W_{23} &= W + b_x \cos(\pi/6 + \phi) - b_y \cos(\pi/3 - \phi), \\ W_{13} &= W - b_x \cos(\pi/6 - \phi) - b_y \cos(\pi/3 + \phi). \end{aligned} \tag{88}$$

Following steps of [95], discussed in previous sections, the MGF of the number of full rotations of the needle is determined by the lowest-real-part eigenvalue and corresponding eigenvectors of (86). While it is not streightforward to study the exact expressions for eigenvectors of a 3×3 matrix, it is not hard to derive lowest cumulants of the rotation numbers by treating the counting parameter χ perturbatively [154]. As in the example of the reversible ratchet, the detailed balance imposes constraints, such that on average the needle rotation becomes a purely geometric phase effect, and consequently, the average number of performed rotations per cycle can be expressed as an integral over the surface **Sc** inside the contour **c** in the (b_x, b_y) parameter space, namely

$$\langle n \rangle = \int\int_{\mathbf{S_c}} db_y db_x F(b_x, b_y). \tag{89}$$

The "Berry curvature" $F(b_x, b_y)$ determines the sensitivity of the system to the external driving. For a symmetric barrier configuration ($\phi = \pi/3$), the expression for $F(b_x, b_y)$ is particularly simple

$$F(b_x, b_y) = \frac{3\sqrt{3} e^{3\sqrt{3}b_x/2 + 3b_y}}{\left(e^{\sqrt{3}b_x/2} + e^{3b_y/2}(1 + e^{\sqrt{3}b_x})\right)^3}. \tag{90}$$

Positivity of the Berry curvature in Fig. 13 means that the maximum number of rotations per one cycle is achieved for the contour that encloses the feature in Fig. 13 from a very large distance in the parameter space. For such a large contour the limits of the integration can be safely set to infinities. The result of the integration in (89) then reads

$$\int_{-\infty}^{\infty}\int_{-\infty}^{\infty} db_y db_x F(b_x, b_y) = 1. \tag{91}$$

This shows that the system in Fig. 12 can make maximum one net rotation on average after the magnetic field rotation along a closed non-intersecting contour, which corresponds to 3 ATP molecules synthesized per one cycle. Note that this result does not require that the coupling to the magnetic field is the largest energy scale in the model. In our calculations we always assumed that $W > b_{x/y}$, in order to use a 3-state approximation; the quantization happens only on average, and the needle is allowed to make many stochastic steps before the rotation of the magnetic field is complete.

Measuring the number of ATP molecules vs the absolute value of the field, one can determine the function $F(b_x, b_y)$. Fig. 13 shows that $F(b_x, b_y)$ has a 3-fold symmetry as the kinetic model, so its measurements can reveal details of the internal molecular structure and possible sub-steps in the effective kinetic model. Interestingly, the theory predicts that the geometric phase and the function in Fig. 13 are independent of the kinetic rate k and the size of an unperturbed barrier W. This means, in particular, that the function $F(b_x, b_y)$ can be robust against variations of the solution viscosity, as long as the magnetic field rotation is adiabatically slow and the system always remains close to the thermodynamic equilibrium. Thus we predict a universality of the motor response, which can be tested experimentally. Beyond the thermodynamic equilibrium, e.g. when a motor is additionally driven by a proton gradient, this property may disappear.

10. Discussion

The analogy between the evolution of generating functions in stochastic processes and the evolution of quantum mechanical wave functions allows to consider complex stochastic processes using the framework of quantum mechanics. In this review we discussed how due to this analogy, quantum mechanical Berry phases appear to have their counterparts in classical stochastic processes. The quantum pump effect, which origin can be traced to the Berry phases, has a stochastic counterpart with a similar geometric phase interpretation. We also showed that like in quantum mechanics, geometric phases can influence the motion of coarse-grained degrees of freedom in stochastic processes after elimination of fast variables. This similarity raises questions about the possibility of further analogies.

For example, Berry phases are responsible for a number of important effects in solid state physics, such as the quantum Hall effect. Currently, it is unclear whether or not similar effects can be discovered in classical dissipative systems, however, several features of the SPE appear to be common with these quantum mechanical phenomena. We discussed that the SPE can be quantized, which originally was considered as a special feature of the quantum pump and the quantum Hall effect, motivating their metrological applications [155]. There are examples of half-quantized responces of stochastic systems [127]. Another example of this kind can be found in the recent work of Rudner and Levitov [156], who discovered the quantization of the dissipative transport of a particle on a periodic lattice with non-Hermitian evolution. Usually quantization is achieved in the limit of the maximum efficiency of the stochastic system response per a cycle in the controled parameter space. While such limits are easy to find in simple models, there is little known about how to determine them in the general case. One possibility was proposed by Shi and Niu in [119]. Examining the diffusion in a periodic potential they related the quantization of the stochastic ratchet current to the Chern number.

Certainly, there are important differences between quantum and classical systems.

The quantum theory of polarization and the quantum Hall effect require the existence of the Fermi sea, and thus are intrinsically many-body effects, relying on the Pauli principle for a multi-particle fermionic wave function. To some extent the Pauli principle can be mimicked in stochastic processes by exclusion interactions, which was used for example in the theory of the shot noise in electronic circuits [98]. It becomes important to explore geometric phases in strongly interacting many-body stochastic systems, such as in reaction-diffusion models and multistate exclusion processes [157, 158]. In quantum field theories Berry phases are responsible for the chiral anomalies [159], playing an important role in the quantum Hall effect, and the quantum pump effect theory [160]. It should be interesting to understand whether effects similar to chiral anomalies can be found in reaction-diffusion processes using the quantum-stochastic analogies discussed in this review. Even in simple systems interactions lead to important effects, such as modifying the no-pumping conditions [122, 127].

Conversely, the quantum theory can benefit from the analogy with stochastic kinetics. For example, one can explore the possibility of a similar to the no-pumping theorem result in quantum mechancis. It is also possible to consider geometric phases in evolution of the counting statistics in quantum mechanical systems [161].

One of the goals of this review was to emphasize that geometric phases can play an important role in the theory of molecular motors. Many studies concentrated on the thermodynamics of molecular machines, with the goal to improve their energy efficiency. However, the work or the entropy production by a molecular motor may not be the most important their characteristics. After all, living cells have plenty of ATP molecules to power their motion. In stochastic environment, when the energy optimization is not crucial, other characteristics such as the accuracy of the performed task, or the simplicity of the structure become most important in designing new molecular machines. We showed that calculations of geometric phases are important to predict molecular motor operations and design them. Measurements of the Berry curvature should provide a new insight into the structures of motor molecules.

While the amount of the theoretical work on the ratchet effect and its applications to molecular machines is by now considerable, simple universal results have been very rare. After the importance of the symmetry breaking and the nonlinear nature of the ratchet effect were recognized, it seemed that there are no more universal rules to predict the size, and even the direction of the induced motion, except by solving corresponding differential equations with time-dependent fields numerically. Such a direct approach becomes extremely complicated when it is applied to a realistic molecular motor. The geometric theory of driven stochastic systems, together with the discovery of the universal exact results such as the pumping-restriction theorems, the fluctuation theorems and the reciprocal relations [134] demonstrated that simple universal laws of molecular machine operations do exist. The future research efforts should demonstrate that such laws can transform the theory of controlled mesoscopic systems.

Acknowledgments

Author thanks Qian Niu and Ilya Nemenman for useful discussions. This work was funded in part by DOE under Contract No. DE-AC52-06NA25396.

References

[1] Berry M V 1984 *Proc. R. Soc. Lond. A* **392** 45
[2] Griffiths D J 2004 *"Introduction to Quantum Mechanics"* Benjamin Cummings; (2nd Edition)
[3] Berry M 1990 *Physics Today* ISSN 0031-9228 **43** 34
[4] Smit J 1955 *Physica* **21** 877
[5] Smit J 1958 *Physica* **24** 29
[6] Sinitsyn N A 2008 *J. Phys.; Condens. Matt.***20** 023201
[7] Murakami S, Nagaosa N and Zhang S-C 2003 *Science* **301** 1348
[8] Sinova J *et al* 2004 *Phys. Rev. Lett.* **92** 126603
[9] R Resta 2008 *J. Phys.: Conf. Ser.* **117** 012024
[10] Shalyt-Margolin A E, Strazhev V I and Tregubovich A Ya 2007 *"Computer Science and Quantum Computing", Nova Science Publishers* 125
[11] Brockett R W 1976 *Proc. IEEE* **64** 61
[12] Murray R M, Li Z and Sastry S S 1994 *"A Mathematical Introduction to Robotic Manipulation"*, CRC Press, Boca Raton
[13] Jarzynski C 1995 *Phys. Rev. Lett.* **74** 1732
[14] Chruscinski D and Jamiolkowski A 2004 *"Geometric Phases in Classical and Quantum Mechanics"* Birkhäuser, Boston
[15] Zwanziger J *et al.* 2003 *"The Geometric Phase in Quantum Systems: Foundations, Mathematical Concepts, and Applications in Molecular and Condensed Matter Physics"* Springer
[16] Stehmann T, Heiss W D and Scholtz F G 2004 *J. Phys.* A **37** 7813
[17] Berry M V and Dennis M R 2003 *Proc. R. Soc. London, Ser.* A **459** 1261
[18] Shuvalov A L and Scott N H 2000 *Acta Mech.***140** 1
[19] Gerrison J C 1988 *Phys. Lett. A* **128** 177
[20] Dattoli G, Mignani R and Torre A 1990 *J. Phys. A: Math. Gen.* **23** 5795
[21] Berry M V 1990 *Proceed. Math. Phys. Sciences* **430** 405
[22] R Schilling, Vogelsberger M and Garanin D A 2006 *J. Phys. A: Math. Gen.* **39** 13727
[23] Klyshko D N 1993 *Usp. Fiz. Nauk* **163** 1
[24] Jordan T F 1988 *J. Math. Phys.* **29** 2042
[25] Vinet L 1988 *Phys. Rev. B* **37** 2369
[26] Benedek C and Beenedict M G 1997 *Europhys. Lett.* **39** 347
[27] Han D, Kim Y S and Noz M E 1999 *Phys. Rev.* E **60** 1036
[28] Han D, Hardekopf E E and Kim Y S 1989 *Phys. Rev.* A **39** 1269
[29] Hannay J H 1985 *J. Phys. A.* **18** 221.
[30] Littlejohn R J 1988*Phys. Rev.* A **38** 6034
[31] Ferraro R and Thibeault M 1999 *Eur. J. Phys.* **20** 143
[32] Mukunda N, Aravin P K and Simon R 2003 *J. Phys. A: Math. Gen.* **36** 2347
[33] Kitano M 1995 *Phys. Rev. A* **51** 4427
[34] Gerry Ch. C 1989 *Phys. Rev. A* **39** 3204
[35] Kitano M and Yabuzaki T 1989 *Phys. Lett. A* **142** 321
[36] Sinitsyn N A and Saxena A 2008 *J. Phys. A: Math. Theor.***41** 392002
[37] Choutri H, Maamache M and Menouar S 2002 *J. Korean Phys. Soc.* **40** 358
[38] Mehri-Dehnavi H and Mostafazadeh A 2008 *J. Math. Phys.* **49** 082105
[39] Mailybaev A A, Kirillov O N and Seyranian A P 2005 *Phys. Rev.* A **72** 014104
[40] Gunther U, Rotter I and Samsonov B F 2007 *J. Phys.* A **40** 8815
[41] Sun C P 1993 *Phys. Scr* **48** 393
[42] Dembowski C *et al.* 2004 *Phys. Rev.* E **69** 056216
[43] Dembowski C *et al.* 2001 *Phys. Rev. Lett.* **86** 787
[44] Landsberg A S 1992 *Phys. Rev. Lett.* **69** 865
[45] Landsberg A S 1993 *Mod. Phys. Lett.* B **7** 71
[46] Ning C Z and Haken H 1991 *Phys. Rev.* A **43** 6410
[47] Ning C Z and Hanken H 1992 *Mod. Phys. Lett.* B **6** 1541
[48] Coullet P, Lega J and Pomeau Y 1991 *Euro. Phys. Lett.* **15** 221
[49] Sinitsyn N A, Dobrovitski V V, Urazhdin S and Saxena A 2008 *Phys. Rev.* B **77** 212405
[50] Frisch T, Rica S, Coullet P and Gilli J M 1994 *Phys.Rev. Lett.* **72** 1471
[51] Rudiger S, Casademunt J and Kramer L 2007 *Phys. Rev. Lett.* **99** 028302
[52] Kawagishi T, Mizuguchi T and Sano M 1995 *Phys. Rev. Lett.* **75** 3768
[53] Vierheilig A, Chevallard C and Gilli J M 1997 *Phys. Rev.* E **55**, 7128
[54] Rudzick o and Mikhailov A S 2006 *Phys. Rev. Lett.* **96** 018302

[55] Scroggie A J, Gomila D, Firth W J and Oppo G L 2005 *Appl. Phys.* B **81** 963
[56] Abarzhi S I, Desjardins O, Nepomnyashchy A and Pitsch H 2007 *Phys. Rev.* E **75** 046208
[57] Maggipinto T, Brambilla M, Harkness G K and Firth W J 2000 *Phys. Rev.* E **62** 8726
[58] Toronov V Yu and Derbov V 1994 *Phys. Rev.* A **50** 878
[59] Toronov Yu and Derbov V L 1997 *Quantum Electronics* **27** 644
[60] Pomeau Y 1971 *Phys. Lett.* A **39** 143
[61] Pomeau Y 2002 *Comptes Rendus Physique* **3** 1269
[62] Spivak B and Andreev V A 2008 *Preprint arXiv:0808.3148*
[63] Malozemoff A P and Slonczewski J C 1979 *"Magnetic Domain Walls in Bubble Materials"* Academic Press, New York
[64] Clarke D J *et al.* 2008 *Preprint arXiv:0806.2383*
[65] Tretiakov O A, Clarke D, Chern G-W, Bazaliy Ya B and Tchernyshyov O 2008 *Phys. Rev. Lett.* **100** 127204
[66] Thiele A A 1973 *Phys. Rev. Lett.* **30** 230
[67] Shapere A and Wilczek F 1987 *Phys. Rev. Lett.* **58** 2051; Shapere A and Wilczek F 1988 *J. Fluid Mech.* **198** 557
[68] Shapere A and Wilczek F 1989 *Am. J. Phys.* **57** 514
[69] Purcell E M 1977 *Am. J. Phys.* **45** 3
[70] Childress S 1981 *"Mechanics of swimming and flying"* Cambridge University Press, Cambridge, New York
[71] Lauga E and Powers T R 2008 *Preprint arXiv:0812.2887*
[72] Avron J E, Gat O and Kenneth O 2004 *Phys. Rev. Lett.* **93** 186001
[73] Najafi A and Golestanian R 2004 *Phys. Rev.* E **69** 062901
[74] Astumian R 2003 *AIP Conf. Proc.* **658** 221
[75] Avron J E, Kenneth O and Oaknin D H 2005 *New J. Phys.* **7** 234
[76] Golestanian R and Ajdari A 2008 *Phys. Rev. Lett.* **100** 038101
[77] Dreyfus R, Baudry J and Stone H A 2005 *Eur. Phys. J.* B **47** 161
[78] Dreyfus R *et al.* 2005 *Nature Lett.* **437** 862
[79] Astumian R D and Dernyi I 2001 *Phys. Rev. Lett.* **86** 3859
[80] Westerhoff H V *et al.* 1986 *Proc. Natl. Acad. Sci. U.S.A.* **83** 4734
[81] Robertson B and Astumian R D 1991 *J. Chem. Phys.* **94** 7414
[82] Robertson B and Astumian R D 1990 *Biophys.J.* **57** 689.
[83] Astumian R D 2005 *J. Phys.:Condens. Matter* **17** S3753
[84] Buttiker M and Moskalets M 2006 *Lect. Notes Phys.* **690** 33
[85] Brouwer P W 1998 *Phys. Rev.* B **58** R10135
[86] Cohen D 2003 *Phys. Rev.* B **68** 155303
[87] Niu Q and Thouless D J 1984 *J. Phys. A***17** 2453
[88] Mottonen M, Vartiainen J J and Pekola J P 2008 *Phys. Rev. Lett.* **100** 177201
[89] Geerligs L G, Anderegg V F, Holweg P A M and Mooij J E 1990 *Phys. Rev. Lett.* **64** 2691
[90] Blumental M D *et al.* 2007 *Nature Physics* **3** 343
[91] Tsong T Y and Chang C H 2003 *AAPPS Bulletin* **13** 12
[92] Kallman E, Healy K and Siwy Z S 2007 *EPL* **78** 28002
[93] Astumian A. D. 2003 *Phys. Rev. Lett.* **91** 118102
[94] Ohkubo J 2008 *J. Stat. Mech.* P02011
[95] Sinitsyn N A and Nemenman I 2007 *Euro. Phys. Lett.* **77** 58001
[96] Sinitsyn N A and Nemenman I 2007 *Phys. Rev. Lett.* **99** 220408
[97] Ohkubo J 2008 *J. Chem. Phys.* **129** 205102
[98] Bagrets D A and Nazarov Y V 2003 *Phys. Rev. B* **67** 085316
[99] Michaelis L and Menten M L 1913 *Biochem. Z.* **49** 333
[100] Sukhorukov E V *et.al.* 2007 *Nature Phys.* **03** 243
[101] Jordan N and Sukhorukov E V 2004 *Phys. Rev. Lett.* **93** 260604
[102] Sukhorukov E V and Jordan A N 2007 *Phys. Rev. Lett.* **98** 136803
[103] Kenzaki H and Kikuchi M 2007 *Proteins: Structure, Function, and Bioinformatics* **71** 389
[104] Aharonov Y and Anandan J 1987 *Phys. Rev. Lett.* **58** 1593
[105] Pati A K 1998 *Ann. Phys.* **270** 178
[106] Sinitsyn N A and Nemenman I 2008 *Technical report, LA-UR-08-04425*
[107] Yarkony D R 1996 *Rev. Mod. Phys* **68** 985
[108] Elgart V and Kamenev A 2004 *Phys. Rev. E* **70** 051205
[109] Pilgram S *et al.*, 2003 *Phys. Rev. Lett.* **90** 206801
[110] Jordan A N, Sukhorukov E V and Pilgram S 2004 *J. Math. Phys.* **45** 4386
[111] Sinitsyn N A 2007 *Phys. Rev.* B **76** 153314

[112] Elgart V and Kamenev A 2006 *Phys. Rev. E* **74** 041101
[113] Sinitsyn N A, Hengartner N and Nemenman I 2008 *Preprint arXiv:0808.4016*
[114] Ohkubo J 2007 *J. Stat. Mech.* P09017
[115] Kagan M L, Kepler T B and Epstein I R 1991 *Nature* **349** 506 ; Kepler T B and Kagan M L 1991 *Phys. Rev. Lett.* **66** 847
[116] Sinitsyn N A and Ohkubo J 2008 *J. Phys. A.: Math. Theor.* **41** 262002
[117] Markin S and R. D. Astumian 1990 *J. Chem. Phys.* **93** 5062
[118] Parrondo J M 1998 *Phys. Rev.* E **57** 7297
[119] Shi Y and Niu 2002 *Europhys. Lett.***59** 2002 324
[120] Mazenko G F 2006 *"Nonequilibrium Statistical Mechanics"* WILEY-VCH Verlag GmbH & Co. KGaA
[121] Lax M 1960 *Rev. Mod. Phys.* **32** 25
[122] Rahav S, Horowitz J and Jarzynski C 2008 *Phys. Rev. Lett.* **101** 140602
[123] Chernyak V Y and Sinitsyn N A 2008 *Phys. Rev. Lett.* **101** 160601
[124] Leigh D A *et al.* 2003 *Nature (London)* **424** 174
[125] Hernandez J V 2004 *et al. Science* **306** 1532
[126] Sauvage J P 2001 "Molecular mashines and motors" *Springer-Verlag* Berlin Heidelberg
[127] Astumian D 2007 *Proceed. Nat. Acad. Sci. U.S.A.* **104** 19715
[128] Jarzynski C 1998 *Acta Physica Polonica* B **29** 1609
[129] Andrieux D and Gaspard P 2007 *J. Stat. Phys.* **127** 107; Astumian R D 2007 *Phys. Rev. E* **76** 020102(R)
[130] Astumian R D 2007 *Phys. Rev. E* **76** 020102
[131] Hill T L 1989 *"Free energy transduction and biochemical cycle kinetics"* Dover Publications Inc, Mineola, New York
[132] Harris R J and Schütz G M 2007 *J. Stat. Mech.: Theor and Exp.* P07020
[133] Astumian R D and Chock P B 1989 *Phys. Rev.* A.**39** 6416
[134] Astumian R D 2008 *Phys. Rev. Lett.* **101** 046802
[135] Kelly S D, Murray R M 1994 *CDS Technical Report 94-014* California Institute of Technology
[136] Bloch A, Crouch P, Baillieul J and Marsden J 2003 *"Nonholonomic Mechanics and Control"* Springer
[137] Alberts B *et al* 2002 *"Molecular biology of the Cell"* Garland (4th edition)
[138] Gelbart W M and Knobler C M 2008 *Physics Today* **Jan.** 42
[139] Kay R E, Leigh D A and Zerbetto R 2007 *Angew. Chem. Int. Ed.* **46** 72
[140] Browne W R and Ferina B L 2006 *Nature Nanotechnology* **1** 25
[141] Gopich I V and Szabo A 2006 *J. Chem. Phys.* **124** 154712
[142] English B P *et al.* 2006 *Nat. Chem. Biol.* **2** 87
[143] Kolomeisky A B and Fisher M E 2007 *Annu. Rev. Phys. Chem.* **58** 675
[144] Rostovtseva T K and Bezrukov M 1998 *Biophys. J.* **74** 2365
[145] Itoh H *et al* 2004 *Nature* **427** 465
[146] Soong R K 2001 *et al., Biomedical Microdevices* **3:1** 71
[147] Kulic I M and Nelson P C 2008 *EPL* **81** 18001
[148] Tsong T Y and Chang C-H 2007 *BioSystems* **88** 323
[149] Hänggi P and Marchesoni F 2008 *Preprint arXiv:0807.1283*
[150] Reimann P 2002 *Phys. Rep.* **361** 57
[151] Jülicher F, Ajdari A and Prost J 1997 *Rev. Mod. Phys.* **69** 1269
[152] Astumian R D and Derenyl I 1998 *Eur. Biophys. J.* **27** 474
[153] Astumian A D and Hänggi P 2002 *Physics Today* **Nov** 33
[154] de Ronde W H, Daniels B C, Mugler A, Sinitsyn N A and Ilya Nemenman 2008 *Preprint arXiv:0811.3283*
[155] Flowers J L and Petley B W 2001 *Rep. Prog. Phys.* **64** 1191
[156] Rudner M S, Levitov L S 2008 *Preprint arXiv:0807.2048*
[157] ChaudhuriA, Jain K, Marathe R and Abhishek Dhar 2007 *Phys. Rev. Lett.* **99** 190601
[158] Marathe R, Jain K and Dhar A 2008 *J. Stat. Mech.* P11014
[159] Bertlmann R A 2005 *Anomalies in quantum field theories* (Oxford University Press, USA)
[160] Andreev A and Kamenev A 2000 *Phys. Rev. Lett.* **85** 1294
[161] Bel G, Zheng Y and Brown F L H 2006 *J. Chem. Phys.* B **110** 19066